# A STUDY OF THE BEHAVIOUR OF THE ROCK MASS SURROUNDING THE VENTERSDORP CONTACT REEF (VCR) AT KLOOF GOLD MINE AIMING AT IMPROVED SUPPORT DESIGN.

GEORGE BOADI QUAYE

A project report submitted to the Faculty of Engineering, University of the Witwatersrand, Johannesburg, in partial fulfillment of the requirements for the degree of Master of Science in Engineering.

Johannesburg, 1997

# DECLARATION

I declare that this project report is my own, unaided work. It is being submitted in partial fulfillment for the Degree of Master of Science in Engineering in the University of the Witwatersrand, Johannesburg. It has not been submitted before for any degree or examination in any other University.

Signature of Candidate

08/09/97

Date

# ABSTRACT

The difference in behaviour of the rock mass surrounding the VCR stopes was believed to be due largely to the different combinations of hangingwall and footwall rock types. The desire to develop a thorough understanding of this behaviour led CSIR, Mining Technology to identify and define of geotechnical areas on all mines exploiting the VCR by CSIR, Mining Technology. The results presented in this report were obtained from one of such geotechnical area on Kloof Gold Mine, where the VCR is overlain by soft lava and underlain by quartzite conglomerate.

The study was carried out in #3 shaft on both the southern and northern sides of the 33/27 longwall at Kloof Gold Mine. The strategies adopted to study the rock mass behaviour included laboratory testing of rock samples, convergence and extensometer monitoring, mapping of mining induced stress fractures and geological features, and the use of a conceptual model to investigate the mechanisms which could be responsible for the observed behaviour. The results obtained from the convergence monitoring indicated that the closure rate is generally less than 5 mm/day and could be attributed to the low face advance rate. The extensometers did not reveal any appreciable separation of bedding-parallel discontinuities in both the hangingwall and footwall strata. Detailed mapping of mining induced stress fractures and geological features showed that the area is highly faulted. Extensive rock falls were noted between the composite timber packs. Stereographic projection of the orientation and inclination of the various discontinuities later revealed that the observed rock falls between the composite timber packs in the area are due largely to the unfavourable intersection of mining induced stress fractures and geological features. Detailed investigation of the distribution and frequency of both geological features and mining induced stress fractures have been seen to be essential for effective support design studies. A slight reduction in strike spacing between support units could help improve the effectiveness of the support system in the northern panels. The test results obtained from the laboratory have been used as input paramaters in a conceptual model to understand some of the mechanisms that could account for the observed behaviour.

# DEDICATION

**To my mum, Abigail and aunt, Esther, with thanks**

***Your prayers have been the source of my inspiration***

# ACKNOWLEDGMENT

I acknowledge my sincerest gratitude to the management of CSIR Miningtek for giving me the opportunity to carry out the task outlined in this report. The objectives of this study wouldn't have been achieved without their enormous support. Words can not just express my thankfulness to my internal supervisor Prof. Mu Ozbay, who after consultation with Miningtek offered me the opportunity to carry out this study. I am also indebted to my external supervisor, Dr. Robin Eve for his constructive criticisms, motivation and invaluable contributions during this study. I am also grateful to Mr. Gokhan Guler for taking me through the intricacies of instrumentation and underground site monitoring. Thanks are due to Dr. Joachim Berlenbach for his guidance and suggestions during the fracture mapping and to Mr. Joachim Schweitzer for his motivation. The names of Dr. John Napier and Dr. Terry Hagan can not be left unmentioned for reading through this report.

I am also indebted to Mr. Deon Geyser, Rodney and Nicole of the Rock Mechanics department at Kloof Gold Mine, for their assistance and kind cooperation during the study. I need to commend Mr. Emmanuel Acheampong and Mr. Kwabena Owusu for their advice and assistance in diverse ways. Finally, I wish to express my appreciation and thankfulness to the entire staff of CSIR Miningtek for the friendly atmosphere I enjoyed during this study.

# TABLE OF CONTENTS

# LIST OF FIGURES

# LIST OF TABLES

# CHAPTER ONE

# INTRODUCTION

## 1.1 Objectives of the study

Different combinations of hangingwall and footwall rock types surrounding the Ventersdorp Contact Reef (VCR) have been identified on most mines exploiting this reef. The various rock types may be characterized by their mechanical properties. These differences in rock properties are believed to give rise to different rock mass behaviour. Sound scientific evidence has not previously been available to affirm this speculation.

The primary objective of this study is to develop a far deeper understanding the rock engineering behaviour of the rock mass surrounding the VCR at depth. This understanding should lead to improved support systems.

## 1.2 Scope of work

This study has been restricted to Kloof Gold Mine on 33/27 longwall in #3 shaft. At this site the VCR is sandwiched between a soft lava hangingwall and a quartzite conglomerate footwall; this combinations of hangingwall and footwall rock types constitute a geotechnical area which has been studied in some detail. The research was conducted on both the southern and northern sides of the longwall. Instrumentation and monitoring of the rate of convergence, detailed investigation of fracture patterns and identification of important geological features associated with the VCR have been carried out. In addition laboratory testing of the soft lava and quartzite was done to determine their respective strength characteristics; these results have been used to determine input parameters for a numerical model. The numerical modelling work is aimed at gaining understanding of some of the mechanisms responsible for the observed behaviour. The results from all aspects of the research are used to construct a conceptual model for the rock mass behaviour in the given geotechnical area. In addition to this conceptual model some recommendations as to suitable methods of support design are suggested.

## 1.3 Structure of the report

In this Chapter the objectives and scope of the study are outlined. Accounts of previous studies on the VCR, found in literature, are reviewed in Chapter 2. Methods used in instrumentating and monitoring of convergence and the results obtained are presented in Chapter 3. Chapter 4 gives a detailed account on the fracture pattern and its relation to geological features. The numerical modelling that was carried out to test the conceptual model derived from the results of Chapters 3 and 4 is discussed in Chapter 5. In Chapter 6 the results obtained are summarized and discussed, and conclusions are drawn. These conclusions include some recommendations for the support of the VCR stopes in the Soft lava-Quartzite geotechnical area.

# CHAPTER TWO

## LITERATURE REVIEW

### 2.1 Introduction

In the South African mining industry previous research geared towards understanding rock mass behaviour around stopes has focused mainly on mining of the Carbon Leader Reef (CLR). A considerable body of literature is now available and some degree of confidence in an understanding of the rock mass behaviour associated with mining such reefs has developed. Unlike the case of the CLR very little has been published concerning an understanding of the rock mass surrounding the VCR. Currently, efforts have been concentrated on this subject by Miningtek and this presentation forms part of the studies being done.

This chapter reviews the findings of some previous research into the behaviour of the rock masses surrounding various deposits. Some of the strategies and methodologies adopted to monitor convergence and strata bed separation are also reviewed. The current understanding of the mechanisms involved in mining induced fracturing around stopes is highlighted. Finally a brief discussion of some of the factors governing effective support design is given.

While little work on rock mechanics aspects of the VCR have previously been carried out some detailed study of the VCR geology has been done. Many of the papers referenced come from the geological rather than the rock mechanics literature.

### 2.2 Geotechnical areas

A project on VCR rock mass behaviour recently completed by CSIR Miningtek, which this study forms a part provided a basis for the determination of geotechnical areas. A geotechnical area refers to a region where different rock types constitute the hangingwall and footwall surrounding the reef, in this case the VCR. Such geotechnical areas have been defined on all South African mines exploiting the VCR. This was done in the belief that there are significant differences between the stope hangingwall and footwall rock mass characteristics and with the expectation that different combinations of rock types in the hangingwall and footwall of this reef result in different rock mass behaviour around stopes. At Kloof gold mine on which this study focuses, the VCR is overlain by soft 'Westonaria' lava and underlain by Elsburg quartzite. For simplicity sake, these are referred to as soft lava and quartzite respectively, throughout the text.

### 2.2.1 Geological nature of the Ventersdorp Contact Reef

Kloof Gold Mine is situated within the Witwatersrand basin on the eastern margin of the Carletonville Goldfield (formerly known as 'The West Wits Line'). Pre-VCR folding and erosion resulted in the unconformable relationship between the VCR and the Central Rand Group, a quartzite-shale sequence (Engelbrecht et al., 1986; Roering et al., 1990). Later studies carried out by Berlenbach (1994) revealed that the plane of the unconformity was subsequently tilted and dips 35-40 degrees southeastwards and undulating bedding parallel faulting is commonly observed. Figure 2.1 below shows the unconformable relationship between the VCR and underlying strata. Berlenbach's studies further established that various structures such as thrust faults are associated with bedding parallel faults and that these may result in duplication of reef; this has a significant influence on mining operations. Berlenbach also observed that where these faults step up into the hangingwall of the mining areas, forming frontal or lateral ramps, they often lead to weak cohesion between the footwall and hangingwall of the fault plane. As a result, they are frequently responsible for the rock falls that occur when the supporting reef is mined.

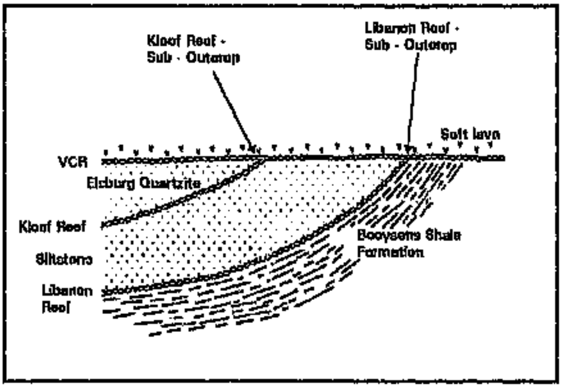


Figure 2.1. The unconformable relationship between the VCR and the underlying strata.

## 2.3 Overview of the behaviour of rock masses surrounding deep level tabular excavations

Deep level tabular excavations are created as a result of mining deep seated tabular orebodies which are deposits having large lateral dimension compared to their width. At such depths, very high field stresses prevail. The act of mining changes this state of stress. These stress changes are referred to as induced stresses, Wagner (1975). Consequently, the resultant stresses acting around the excavation are equal to the sum of the induced and field stresses. Intense fracturing of the rock mass surrounding the excavation is a common feature associated with deep level mining. Es[illegible] by Wagner (1975) revealed that the failure of rocks around excavations is g[illegible] resultant stresses while the displacements may be attributed mainly to the [illegible]sses. The stress and displacement distributions and the associated en[illegible] und such excavations have been analyzed and reported in great detail [illegible] Salam[illegible] These fundamental results improved the understanding of the consequent changes in the gravitational potential energy brought about by the volumetric convergence of underground excavations.

The quest to develop a further understanding of the factors which contribute to the observed characteristics of the rock mass as it deforms urged later researchers to investigate further (Anon, 1988). Past studies have confirmed that the degree of deformation depends upon rock mass characteristics such as the elastic modulus, the nature and frequency of geological discontinuities and fracturing, and upon excavation characteristics such as the depth, span and mining geometry.

### 2.3.1 Monitoring of rock mass behaviour

There are two basic measurements made on mine roofs to determine stability; roof to floor elastic movements (convergence) and the opening of fracture and bedding planes within the strata (hangingwall and footwall bed separation known as inelastic closure).

2.3.1.1 Convergence of underground excavations

Among the earlier workers who endeavoured to determine the factors contributing to convergence around underground excavations was Salamon (1974). He carried out a detailed mathematical analysis to determine the total displacement induced around mining excavations. Later researchers like Wagner (1976) summarized his results. The analysis was carried out by considering a parallel-sided longwall, that constitutes two parallel diverging stopes. A section along strike through such a stope is illustrated figure 2.2 below.

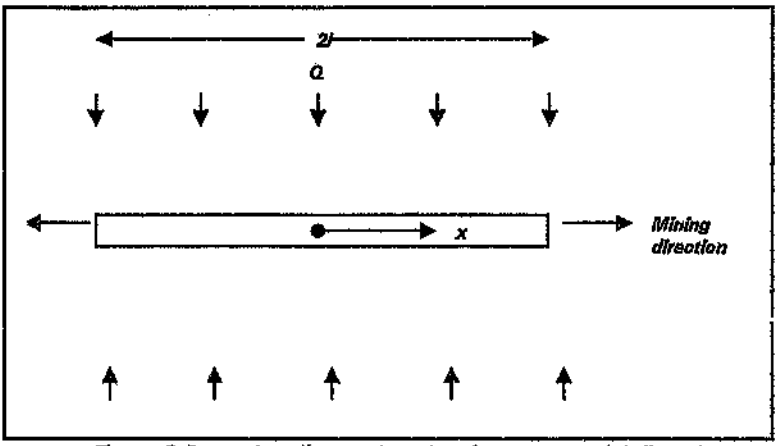


Figure 2.2. A strike section showing two parallel diverging stopes.

Assuming elastic behaviour, convergence at a point x in figure 2.2 is given by Salamon (1974) as:

$$S = \frac{2(1-\nu)Q}{G}\left(l^2 - x^2\right)^{1/2}$$

Where l is half stope span and v is the Poisson's ratio. G is the modulus of rigidity and x is the distance measured from the centre line of the longwall to the point in the mined-out area where convergence is being determined. Q is the vertical component of the virgin stress.

Hawkes and Kwitowski (1979) in an attempt to simplify the observed characteristics of the rock mass behaviour surrounding underground excavations explained that when rock is excavated in underground mining operations, the static stress distribution around the excavation is redistributed. The vertical stresses on the roof and the floor and the lateral stresses on the side (pillar) walls are removed and, to maintain equilibrium the rock subsides, the floor heaves, and the side walls bulge out. These movements, according to Hawkes and Kwitowski, are usually very small and take place during the actual excavation operations, so they are rarely, if ever measured. They further allege that subsequent movements of the excavation are brought about by a combination of two factors i.e. workings in adjacent strata, which causes a further redistribution of the stresses, and creep, associated with fracturing of the rock in the roof, floor and sides (pillars) of the excavation.

Subsequent contributions by Gurtunca et al (1989) stated that the convergence measured underground has three components. These are elastic convergence, inelastic bed separations and closure due to dilation. They described the elastic convergence as the elastic relaxation of the rock mass in response to mining. The inelastic bed separations take place very close to the face where the first few layers in the hangingwall displace downwards due to their own mass. The contribution due to dilation in the rock mass ahead of the face, as proposed by Brummer (1987) and quoted by Gurtunca et. al (1989), is due to shear movements along bedding planes and extension fracturing. These generate vertical displacements and horizontal compressive forces, which in turn cause the strata to deform into the stope.

### 2.3.2 Hangingwall and footwall bed separation measurements

Hawkes and Kwitowski (1979), give a detailed description about modern measuring devices for monitoring hangingwall and footwall bed separation. These measurements are made between an anchor point in a borehole and a point near the mouth of the borehole. Recently, instruments have been developed to monitor deformations between successive anchor points in the borehole and a typical example is the one adopted in this study. It is described in Chapter 3. The purpose of measuring between the immediate roof and different points along a borehole is to determine at which horizon movements are taking place. It can not be assumed that all movements represent dilation of the strata because many cases have been reported in which open fractures actually close during roof settlement (Hawkes and Kwitowski, 1979). The amount of hangingwall and footwall bed separation that can be measured using this method is ultimately limited by borehole shearing. Once the strata have sheared along a bedding or fracture plane to the extent that the anchor connectors are trapped, further measurements become meaningless.

### 2.3.3 Mining induced stress fracturing around deep level tabular excavations

Underground mining operations have been observed to induce large stress concentrations immediately in front of stope faces. These stresses result in intense and characteristic patterns of fracturing. Over the years, several researchers (Cook, 1962; Hoek and Bieniawski, 1966; Fairhurst and Cook, 1966; Hodgson, 1967; Kersten, 1969; Adams and Jager, 1979) endeavoured to understand the fracture patterns and mechanisms causing their formation around stopes. Despite the fact that their results did not yield a full understanding of the principles involved, it paved a way for subsequent researchers to carry out further investigations, the mechanisms associated with fracturing around stopes.

In an attempt to simplify their observations of mining induced fracturing around deep gold mine stopes Brummer et al. (1984) took into account views of some previous researchers, who had proposed that there are two types of fractures around stopes. These are extension fractures and shear fractures. The extension fractures form parallel to the direction of the maximum principal stress when the minimum principal stress is low. The shear fractures comprise of many closely spaced extension fractures but which have the overriding common characteristics of permitting relative lateral movement between the intact rock on either side of the overall shear zone.

A later investigation by Legge (1986) confirmed that the primary fracturing (shear fractures) occur several metres ahead of an advancing stope face whereas secondary fracturing (extension fractures) occurs close to the stope face. According to Brummer (1984) the onset of shear fracturing in the region ahead of an advancing stope face is as a result of shear failure of the rock due to the relatively high stresses in that region. This brings about the formation of conjugate shear fracture planes near the reef plane. These planes form at fairly regular spacing. Brummer further explained that horizontal parting planes then facilitate the dilation of the failed rock towards the mined out area, and the horizontal stress at a point on the reef plane is therefore reduced as the face is advanced. This reduction in the minimum principal stress as the face approaches a point causes most of the formerly solid regions between shear fractures, to fracture in a brittle or extension fashion parallel to the maximum principal stress. The combinations of face-parallel shear/extension fractures and parting planes have been observed to break the hangingwall strata into distinct blocks that could result in falls of ground.

Adams and Jager, 1979; Gay and Jager (1986) also identified four sets of extension and shear fractures in stopes. Their observations revealed that all the fractures are orientated parallel to the stope face with a variation of ±10 degrees. The various types of fractures are distinguished by their dip and surface characteristics. Specifically, the shear fractures constitute a shear zone filled with communited material. Extension fractures on the other hand are clean fractures exhibiting little or no ride displacements (Anon, 1988). They usually terminate abruptly on parting planes.

## 2.4 Stope support design

Quite an appreciable effort has been centered on the development of stope support technology over the years. Emere (1982) is one such worker who has published his findings and recommendations within a mining depth range of 500-2000 metres. Jager and Roberts (1986) extended Emere's studies to greater depths. They concluded that, the design of a support system depends on an understanding of the following:

(i) The mechanism of inelastic closure.

(ii) The self-supporting nature of the hangingwall layers.

(iii) The interaction of support units with fractured beams.

(iv) The interaction of seismic waves with the fractured and layered rock around the stope.

Requirements common to support systems for any depth are that they should have a high initial stiffness and be installed as close to the face as possible. Other important factors that must be considered in the selection of support are the intensity and orientation of fractures, the presence of geological discontinuities, weak strata and the stoping width. These factors influence the spacing, size and type of support to be used (Anon,1988).

### 2.4.1 Review of factors governing the design of stope support systems

Putting the conclusions of Jager and Roberts (1986) together, the design of effective stope support systems depends upon knowledge of three fundamental aspects. These include the nature and extent of the rock to be supported. Others are the deformations to which the support system will be subjected (normally defined by the stope closure profile), and the generated force (load reaction characteristics) of the support systems available for installation (Anon, 1988). These have been summarized in figure 2.3 below.

#### 2.4.1.1 Rock mass to be supported

The immediate rock mass surrounding deep level tabular excavations is usually highly fractured due to the high stresses prevailing at depth. The dilation of this fractured zone causes high compressive horizontal stresses in the stope hangingwall. According to Jager and Roberts (1986), these horizontal stresses clamp the fractured rock together, so that the hangingwall is to a large extent self supporting. However, unfavourable orientations of fractures in the immediate hangingwall may divide it into a set of definite blocks. Some of these may be keyblocks supporting adjacent fragmented rock. The situation can be aggravated in cases where complex patterns of mining induced fractures occur together with geological discontinuities.

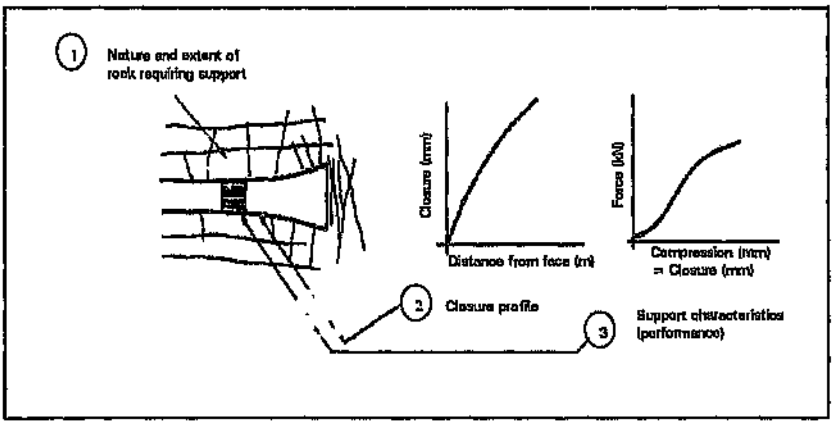


Figure 2.3. Aspects governing stope support design (source: An Industry Guide to Methods of Ameliorating Rockfalls and Rockburst hazards)

Thus it can be deduced that an important factor requiring consideration in the design of effective support system is the nature, orientation and frequency of geological discontinuities (faults, joints etc.). A strike section across a typical deep level rock mass surrounding a stope is shown in figure 2.4 below.

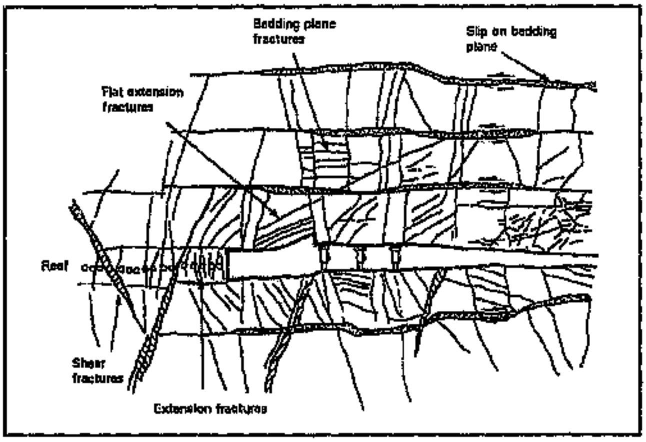


Figure 2.4. The rock mass surrounding a deep stope (source: An Industry Guide to Methods of Ameliorating Rockfalls and Rockburst hazards)

2.4.1.2 Rock mass deformation

Stope support units while undergoing deformations imposed upon them by the surrounding rock mass generate reactive loads to support the immediate hangingwall. The design of a support system therefore requires detailed knowledge about the quasi-static deformations due to elastic and inelastic relaxation of the rock and ride in the stope. Additional information about dynamic (rockburst) deformations is also vital to enhance the choice of a support system with the appropriate yieldability.

2.4.1.3 Support reaction

When the stope hangingwall is supported, the deformation of the surrounding rock mass is imposed on the support unit. To counteract this action, the support units develop reaction forces (loads) which support the hangingwall. The initial forces generated by these units must be high enough to maintain the integrity of the hangingwall beam between adjacent support units and between the support units and the face. In the case of low stope closure rate, active supports have been suggested because of their ability to take up load soon after installation.

In deep level stoping the function of support is primarily to maintain the integrity of the lowermost hangingwall strata and not to support the weight of a large thickness of strata. It is therefore essential to know the force-compression response of the various support types when installed underground in order to evaluate support systems. Figure 2.5 shows a performance curve of a typical support unit.

## 2.5 Stope support and seismicity

When an excavation is made in a rock mass (assumed to be elastic), the rock above the excavation moves downward under the influence of gravity by an amount equal to the volumetric closure of the excavation. There is no net movement of the rock below the excavation. As a result a change in the gravitational potential energy occurs equal to product of the primitive stress and the volumetric closure of the excavation. Some of the gravitational energy appears in the form of strain energy in induced stress concentrations in the rock and the remainder is released. The energy released is dissipated as kinetic energy, in heating the rock mass and in creating additional fracturing of rock around the excavation.

Various attempts have been made in the past to determine the most suitable support system that could help control the rockburst hazard in deep level gold mines. In a study conducted by Jager et al (1987), to determine the relative ability of backfill and other support systems to counteract the kinetic energy imparted to the rock by seismic ground motion, it was concluded that backfill is superior to the other support types in absorbing seismically generated energy. Gurtunca et al (1989) found that the reduction of convergence during rockbursts in filled stopes is considerable compared to conventionally supported stopes and that closure rates are significantly lower in filled stopes than in unfilled stopes. The volumetric convergence of a deep level excavation contributes to the change in gravitational potential energy of the rock mass due to mining a horizontal or near horizontal reef. Hence a reduction in the volumetric convergence results in decreased total potential energy change. Consequently, all quantities involved in the energy build up prior to a seismic event are reduced.

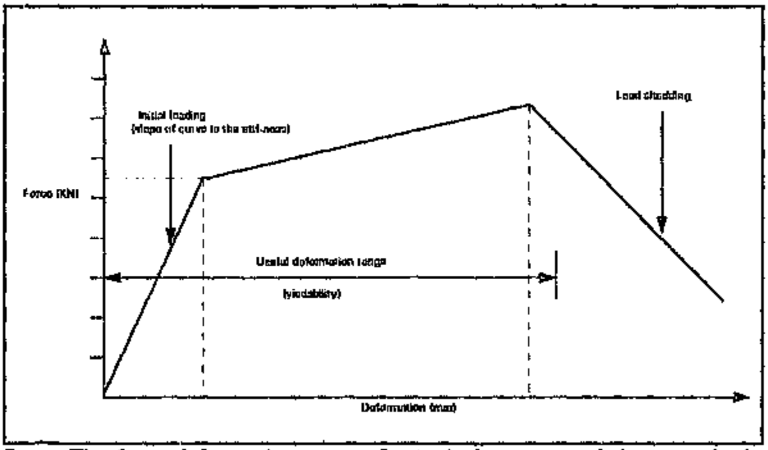


Figure 2.5. The force-deformation curve of a typical support unit (source: An Industry Guide to Methods of Ameliorating Rockfalls and Rockbursts hazards)

## 2.6 Application of numerical modelling

The current state of technology has facilitated the development of computer programmes capable of simulating the behaviour of rock masses surrounding underground excavations. Cundall (1986) developed FLAC (Fast Lagrangian Analysis of Continua). This is a two-dimensional explicit finite difference code for simulating the behaviour of structures built of soil, rock or other materials which may undergo plastic flow when their yield limit is reached. The method has been adopted by Miningtek to model the multi-material rock mass surrounding a stope.

# CHAPTER THREE

## UNDERGROUND SITE MONITORING

### 3.1 Introduction

As part of the efforts by Miningtek to study the rock mass behaviour surrounding the VCR, so as to improve support design, a geotechnical area was defined on Kloof Gold Mine. Various methods were adopted to provide the relevant information about the behaviour of the rock mass. These include detailed underground site monitoring programmes, laboratory testing of rock samples, seismic data analyses and application of various numerical modelling techniques.

This chapter focuses on the convergence monitoring. It begins with a brief discussion on the location of the mine. An account of the instrumentation of the site is given. Graphical presentations and analyses of the results obtained are shown. Finally, deductions arising from the study are presented.

### 3.2 Location of Kloof Gold Mine

The mine is situated in the magisterial district of Westonaria, about 48 kilometers west of Johannesburg. This is illustrated in figure 3.1.

### 3.3 Description of underground monitoring site

The monitoring site was located at an approximate depth of 2.8 km below the earth's surface at Kloof 3 shaft, 33 level, 27 longwall. The footwall comprises Elsburg quartzite overlain by a soft lava hangingwall. Figures 3.2 and 3.3 show the VCR hangingwall and footwall respectively on Kloof Gold Mine. The average dip of the VCR in these stopes is about 30 - 35 degrees towards south-east. The mining configuration adopted is mainly overhand with the stopes advancing along strike. The main permanent support type used to maintain the hangingwall integrity is composite packs. These were installed at an average spacing of 1.8 m (skin to skin) both along strike and dip. Two rows of hydraulic props constituted the face area support.

Monitoring first started in the first and second panels on the southern longwall but came to a halt in February 1995 when production ceased due to very low grade and poor hangingwall conditions. A stabilizing pillar was delineated and the mining was permanently stopped. In order to provide information about increasing stope span on convergence rate, a decision was taken to monitor additional panels namely numbers third and fourth (see figure 3.4). The reasons stated above again compelled the mine authorities to freeze mining operations in these lower panels around October 1995 which led to subsequent instrumentation of 34 level, 27 longwall, first panel.

To achieve a more realistic idea about convergence rate, the first and second panels on the northern side were equipped with measuring devices (see figure 3.5). These three panels were monitored up to August 1996.

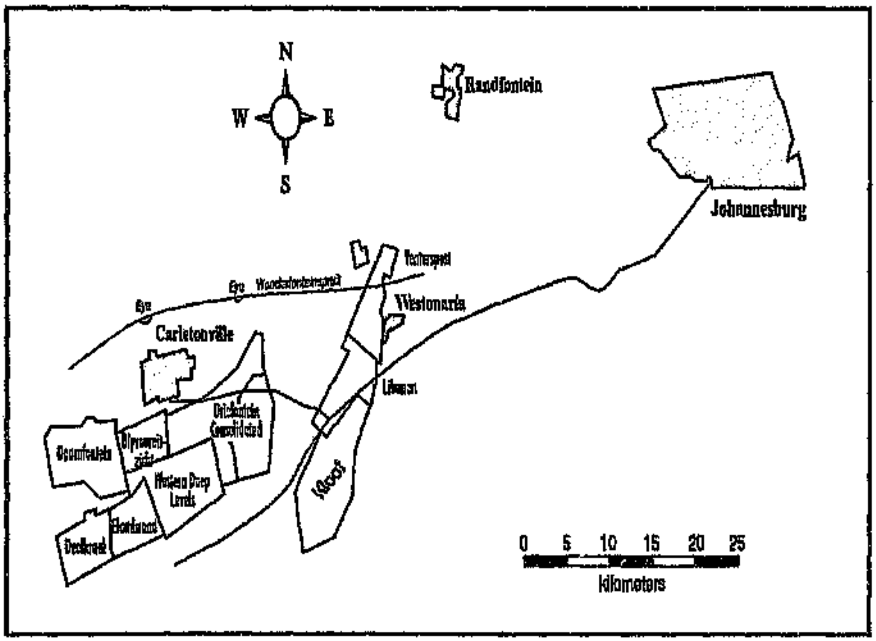


Figure 3.1. Location of Kloof Gold Mine with respect to other gold mines in the Carletonville area.

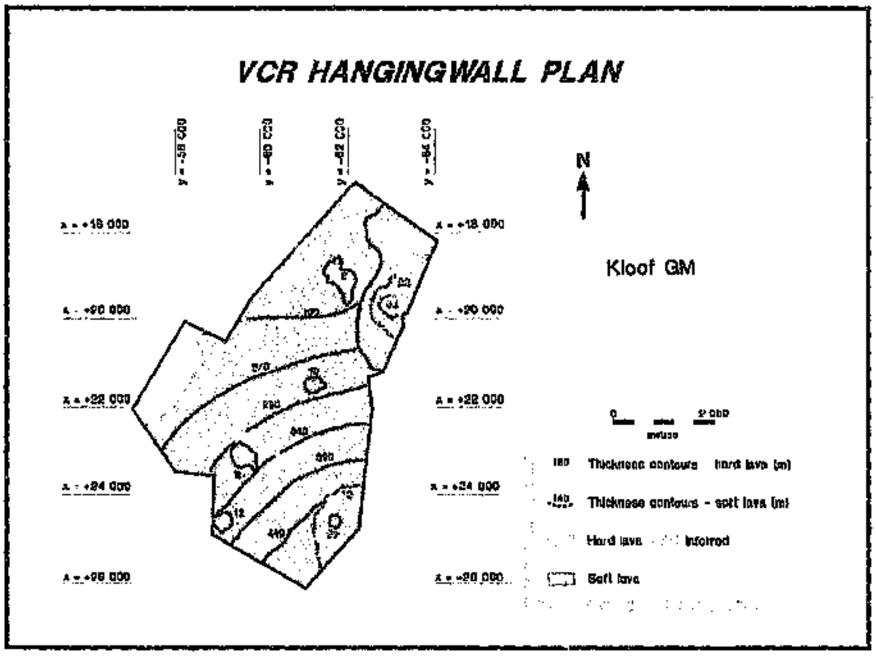


Figure 3.2. VCR hangingwall plan at Kloof Gold Mine.

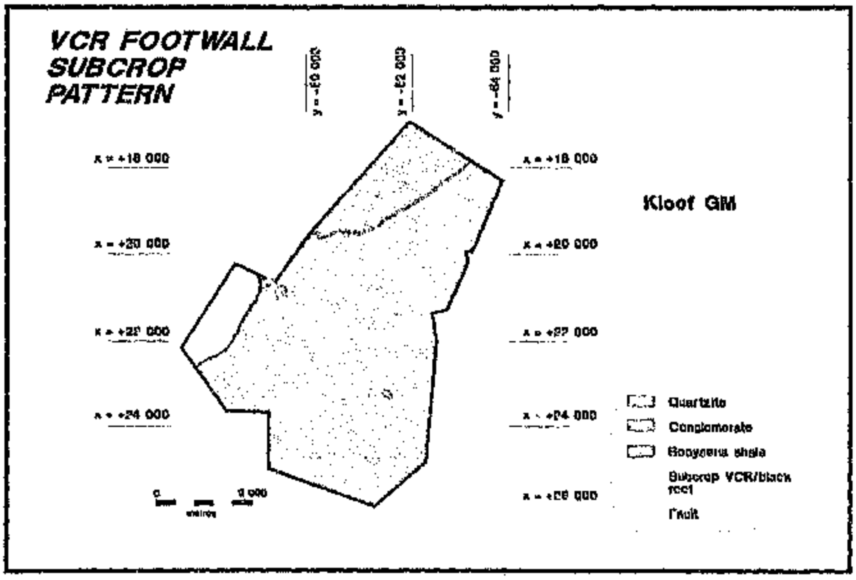


Figure 3.3. VCR footwall plan at Kloof Gold Mine.

## 3.4 Convergence monitoring

Convergence measuring devices were installed in each of the monitoring stopes to determine the normal component of the relative displacement of the footwall and hangingwall. The procedure outlined in the following subsection was adopted to install each of these stations.

### 3.4.1 Installation of convergence monitoring stations

The following description is made with reference to figures 3.4 and 3.5. Three pegs were installed in the hangingwall forming an approximate right angle triangle. This triangle shall be referred to as a base triangle in subsequent sections. Depending on the ground conditions, this was preferably established in the same rock type that was free from exposed discontinuities. This was done so as to prevent the results being affected by the relative movement of adjacent blocks as they slide past each other. The three points of the base triangle were designated as $h_1$, $h_2$ and $h_3$ respectively as shown in figure 3.6. With the aid of a clino- rule the distances labelled b1 and b3 were each kept at 1000 mm. These together with the length of the hypotenuse, b2 were recorded as the base distances respectively.

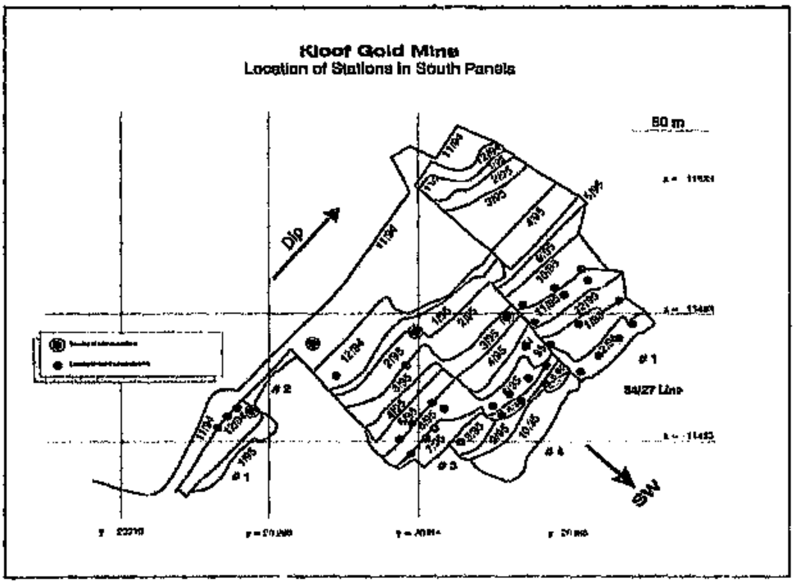


Figure 3.4. Location of underground monitoring stations in 33/27 line, South panels.

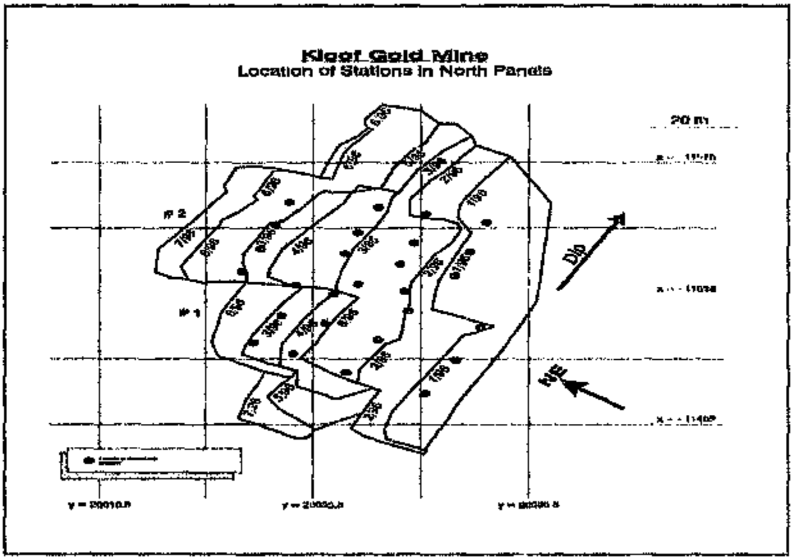


Figure 3.5. Location of underground monitoring stations in the 33/27 line, North panels.

A portable hand-held drill powered by a rechargeable battery was used to create holes 100 mm long and about 10 mm in diameter at each of the three points of the base triangle. Roofbolts were then hammered in place leaving a hook (which an integral part of the bolt) protruding from the collar of the hole. This was used to connect a spring vernier to the roofbolt for measuring purposes. A broken piece of rock was dropped by gravity from the apex of the base triangle ($h_2$) to locate the position of a footwall peg. This peg was also equipped as described.

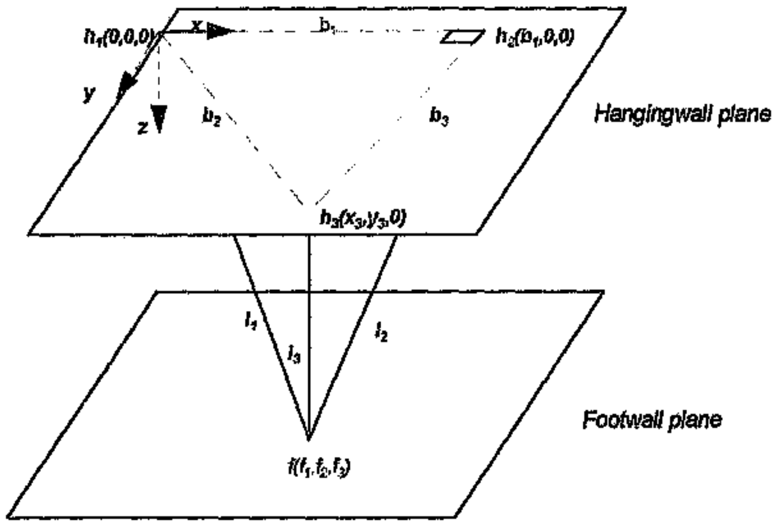


Figure 3.6. Schematic representation of hangingwall and footwall monitoring pegs.

The above method was used to establish three stations approximately in line along dip as shown in figure 3.6. Specifically, each of these stations was positioned at the top, middle and bottom of the panel respectively. These constituted temporary stations because of the inaccessibility of the back areas of the stope with time. This line of temporary stations was extended across the top gully to locate the position of a permanent station. Figure 3.7 below illustrates the above description.

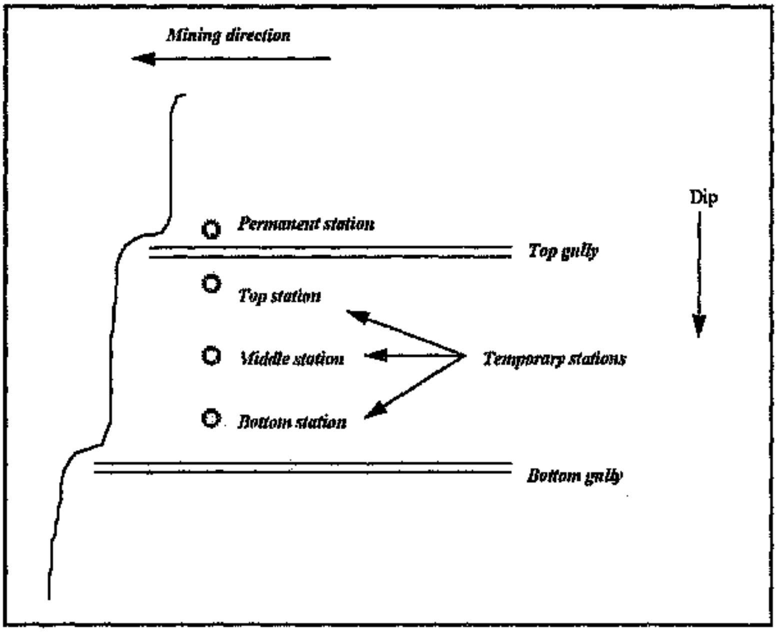


Figure 3.7. Schematic representation of the location of temporary and permanent stations.

### 3.4.2 Calculation of convergence using the 'four peg method'

After installation, the three distances between the hangingwall and footwall pegs were measured. The new position of the footwall peg was found from the following equations (after Piper and Gurtunca, 1987):

The temporary variables $x_3$ and $y_3$ can be calculated from :

$$x_3 = \frac{\left(b_1^2 + b_2^2 + b_3^2\right)}{2b_1}$$

$$y_3 = \sqrt{\left(b_2^2 - x_3^2\right)}$$

The new coordinates of the footwall peg was deteremined as follows:

$$f_1 = \frac{\left(b_1^2 + l_1^2 - l_2^2\right)}{2b_1}$$

$$f_2 = \frac{\left(l_2^2 - l_3^2 - b_1^2 + x_3^2 + y_3^2 + 2f_1\left(b_1 - x_3\right)\right)}{2y_3}$$

$$f_3 = \sqrt{\left(l_1^2 - f_1^2 - f_2^2\right)}$$

Hence on the day of installation the footwall peg coordinate $f_3$, was calculated from the above formulae. Denoting the coordinates on any particular day after installation by $f_3^n$, the amount of convergence n days after installation was computed as:

$$C_n = f_3^n - f_3$$

Using a similar approach, the dip and strike rides, n days after installation were computed from the following equations respectively:

$$D_n = f_1^n - f_1$$

$$S_n = f_2^n - f_2$$

Where $f_1^n$ is the numerical value of the coordinate $f_1$ computed n days after installation. Similarly, $f_2^n$ represents the numerical value of the coordinate $f_2$ computed n days after installation. $f_1$ and $f_2$ represent the respective coordinate on the day of installation.

### 3.4.3 Analysis of results

The formulae outlined above produced results of the rate of convergence. These have been presented graphically in figures 3.8 - 3.10. The curves give an ind... on that the convergence rate as monitored in this geotechnical area has two parts. The first part of the curve depicts a steady increase in convergence with time. However, after about 40 days from the date of installation, the curve assumes a flatter gradient suggesting a reduced rate of convergence. If a face advance rate of 5 m/month (typical of Goldfield mines) is assumed, it can be deduced that this reduced rate of convergence starts when the face position is at about 6.7 m from the monitoring station. Other results obtained have been presented in appendix one, diagrams 1 to 6.

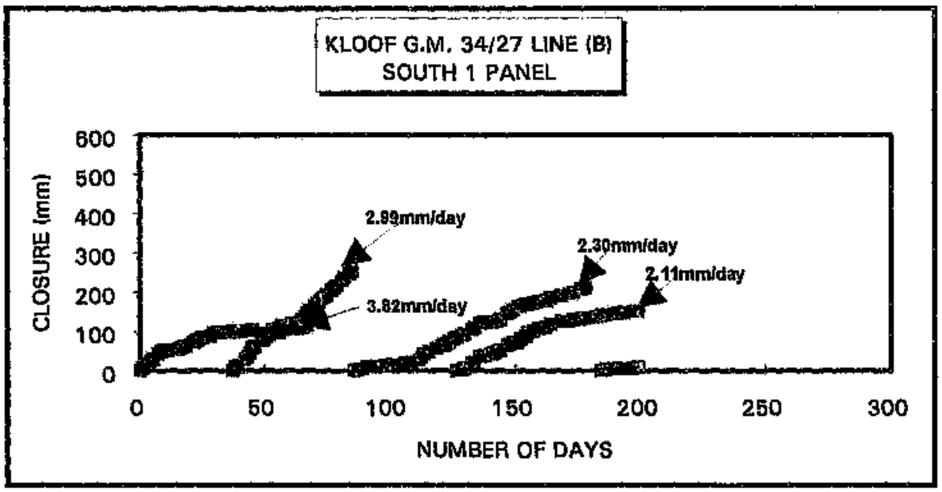


Figure 3.8. Convergence results from 34/27 line, south 1 panel.

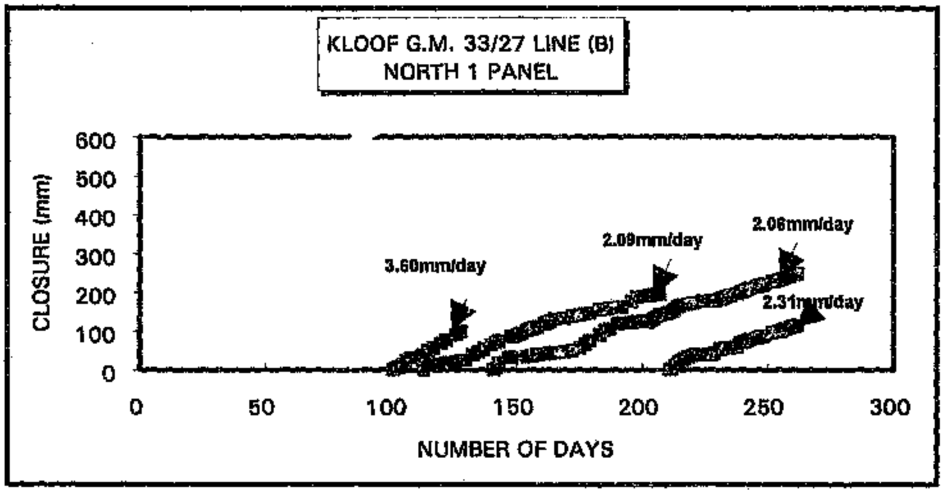


Figure 3.9. Convergence results from 33/27 line, north 1 panel.

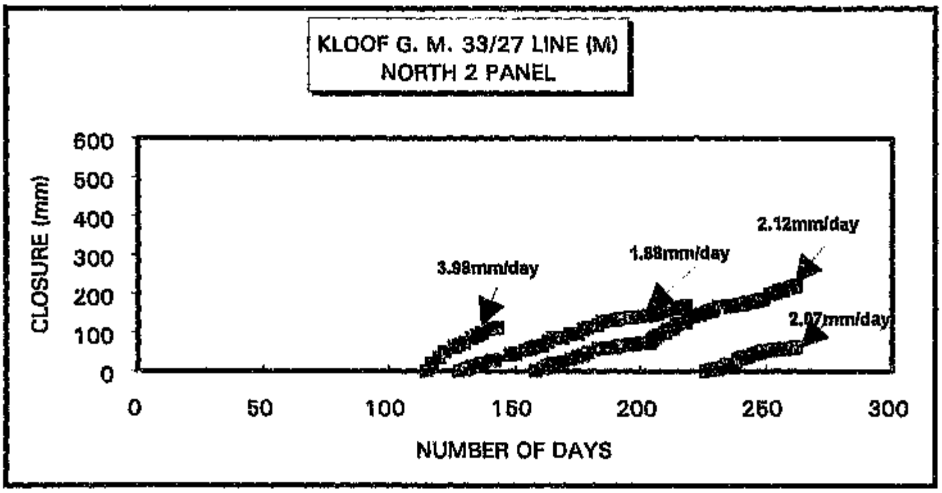


Figure 3.10. Convergence results from 33/27 line, north 2 panel.

#### 3.4.4 Deductions from convergence results

A summary of the results obtained has been presented in table 3.1 below. The convergence measurements obtained during the initial stages of the monitoring programme in the south panels showed high variability with values averaging between 0.45-8.77 mm/day. Values ranging between 5.0 - 9.0 mm/day were recorded when the face was advancing. The lower values could be attributed to the fact that mining was halted permanently and the recorded convergence rates during the period were due to creep effects and mining on adjacent panels. The results from the last three panels showed slight variation between 2.0 - 4.0 mm/day.

It can therefore be deduced that convergence rates in this geotechnical area are very low due to the low rate of face advance. The resistance developed by the permanent support units tends to slow down the rate of convergence when the face position is at about 6.7 m from the support unit.

Table 3.1. Summary of results obtained from all the convergence monitoring stations.

| Panel | Top station average (mm/day) | Middle station average (mm/day) | Bottom station average (mm/day) | Permanent station average (mm/day) |
|---|---|---|---|---|
| 33 South 1 | - | 0.9 | 0.7 | - |
| 33 South 2 | - | - | - | 0.8 |
| 33 South 3 | 2.3 | 2.8 | 3.1 | 2.0 |
| 33 South 4 | 1.8 | 3.6 | 4.2 | 1.0 |
| 34 South 1 | 2.5 | 2.7 | 2.8 | 3.8 |
| 33 North 1 | 3.0 | 2.6 | 2.5 | - |
| 33 North 2 | 2.8 | 2.5 | 2.3 | 2.5 |

## 3.5 Extensometer measurements

In order to quantify the degree of separation between probable bedding parallel discontinuities in the hangingwall and footwall, extensometers were installed along the strike gullies. The locations of the monitoring stations have been shown in figure 3.5. Basically a 10 m long hole having BX inner diameter of 60.3 mm was drilled vertically into the hangingwall. A borehole camera was inserted into the hole to examine the horizons at which bedding parallel discontinuities exist in the strata. An extensometer wire measuring 10.25 m long was attached to an anchor through connecting rods and cautiously pushed into the borehole. The remaining 250 mm of the wire protruded from the collar of the hole into the excavation. A similar approach was adopted to install four other devices at 2 m intervals in the borehole. A 10.25 m long hole in the footwall was equipped in a similar manner. Measurements were taken daily and the amount of separation of bedding parallel discontinuities were computed as shown in figure 3.11:

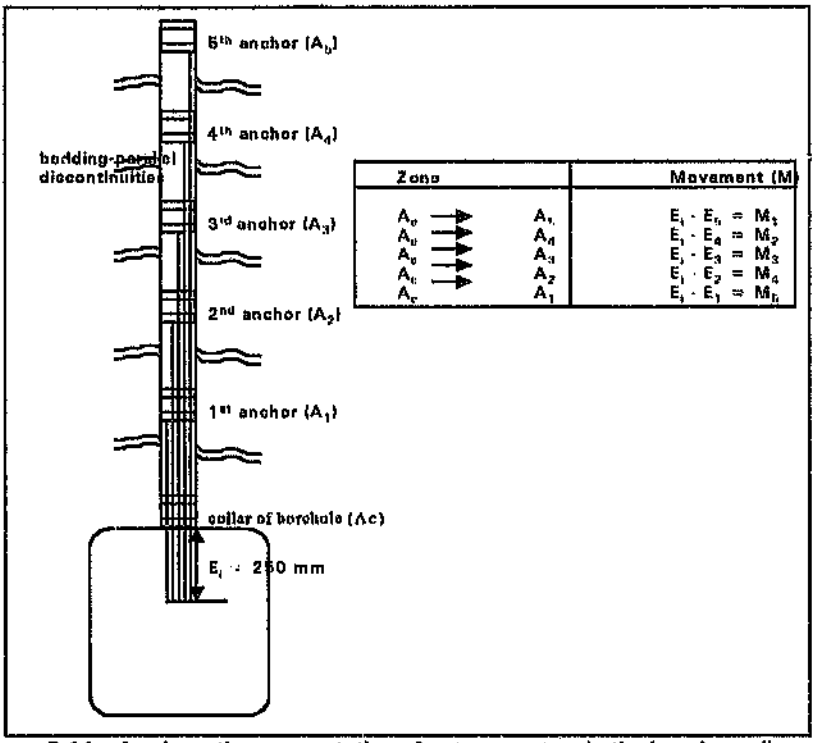

Figure 3.11. A schematic representation of extensometers in the hangingwall.

$M_n$ is the amount of lengthening or shortening measured by the nth extensometer, $E_i$ is the base reading taken on the day of installation and $E_n$ is the measurement recorded by the nth extensometer. Some of the results obtained along number 2 gully in the southern stopes have been presented in the figures 3.12a, b and c. Figures 3.12a and b are results from the hangingwall and figure 3.12c shows results from the footwall.

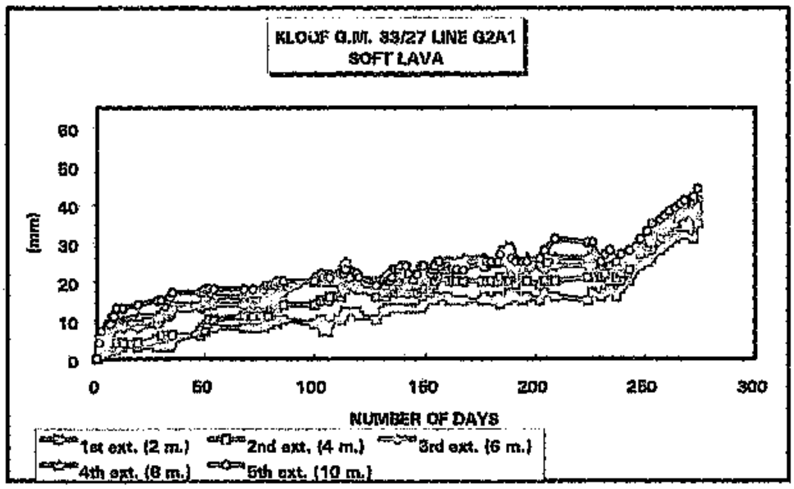
KLOOF G.M. 33/27 LINE G2A1
SOFT LAVA
(mm)
NUMBER OF DAYS
1st ext. (2 m.)
2nd ext. (4 m.)
3rd ext. (6 m.)
4th ext. (8 m.)
5th ext. (10 m.)

(a)

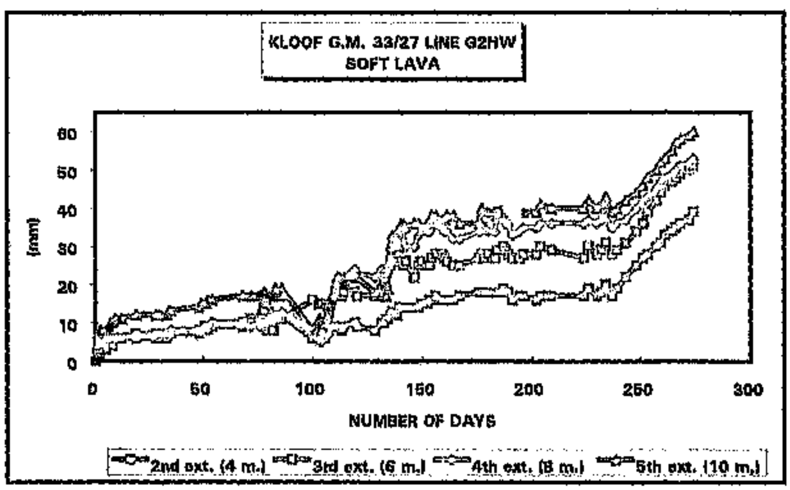
KLOOF G.M. 33/27 LINE G2HW
SOFT LAVA
(mm)
NUMBER OF DAYS
2nd ext. (4 m.)
3rd ext. (6 m.)
4th ext. (8 m.)
5th ext. (10 m.)

(b)

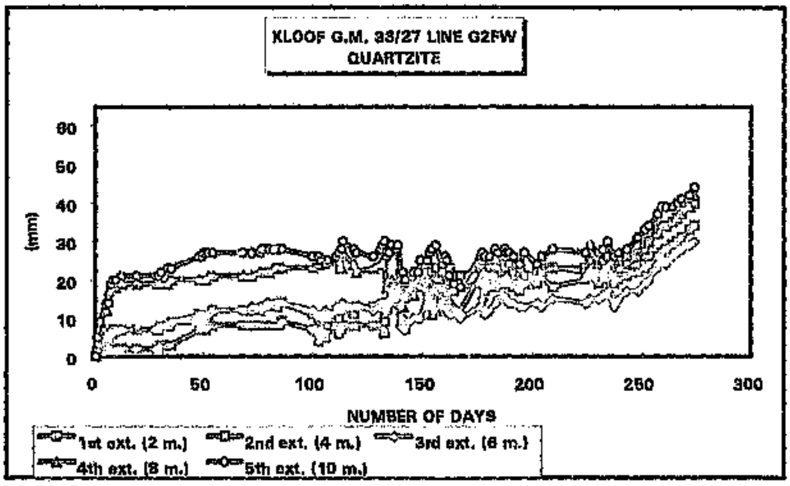


(c)

Figure 3.12. Extensometer results from Kloof Gold Mine, 3 Shaft on 33 Level 27 Line in South 2 panel.

Other results obtained from the extensometers are presented in appendix one, diagrams 7 to 9. No appreciable separation of discontinuities was detected in the soft lava hangingwall and quartzite footwall until after about 240 days. The results obtained during 100 to 240 days after installation were inconsistent and quite different from expectations. The undulating trends of the curves illustrate the complex behaviour of the rock mass (see appendix 1, diagrams 7 to 9). The seismic records for and after this period did not show any increase in seismic activity and therefore this behaviour was thought to be due to creep effect since there was no mining operations at the time. However, the results give an indication that the total convergence in the stopes, are due to partial contributions from both the hangingwall and footwall.

# CHAPTER FOUR

## FRACTURE MAPPING

### 4.1 Introduction

The mode of fracturing of the rock mass surrounding underground excavations is regarded as an essential piece of information for effective support design. Deep underground excavations are usually surrounded by an envelope of fractures, that causes stability problems. As has been outlined in previous chapters, the primary objective of any support design is to maintain the integrity of the immediate hangingwall. When this objective is achieved, it ensures the accessibility of the working area and, more importantly, reduces the number of rock-related accidents. This dual function of support elements can however not be accomplished in isolation. It requires the consideration of both, the degree of fracturing around the stope and the presence of geological features like parting planes, joints and faults. Ignoring this fundamental requirement could result in the ejection of unstable keyblocks which, if not supported, could result in a rock-related accident.

As part of the strategies adopted to improve the understanding of the rock mass behaviour surrounding the VCR, a study of the fracture pattern of the soft lava overlying this reef at Kloof Gold Mine was considered to be essential. This was carried out on 33/27 longwall north and south panels. This chapter represents a summary of the observations made, emphasising the need to consider both, fracture patterns and geological structures. Orientation analysis has been used to present the collected data and photographs to substantiate these findings have been included.

### 4.2 Geological features

The long and complex tectonic history of the Witwaterand basin (e.g. Roering and Smith,1987) has resulted in a complex fault and dyke pattern, which significantly influences the distribution of orebodies and impacts on rockmass behaviour. A detailed discussion of the tectonic history of the Witwatersrand basin is beyond the scope of this study. However, Berlenbach (1995) has shown that faults associated with a northeastward thrust event have had an important influence on the rockmass behaviour at Kloof gold mine. This thrust event postulates an older, northwestward verging thrust event, resulting in a complex reactivation of fault structures. Because faulting has an important impact on rockmass behaviour in the study area, a brief discussion of the fault geometries and mechanisms is given.

Ramsay and Huber (1987) define faults as fracture discontinuities in a rock along which a significant differential displacement (> 0.5 mm and generally much larger than this minimum value) has taken place. Based upon the orientation of the fault plane and the differential movement across it, faults have been classified as normal, reverse and strike-slip faults. The geometric features of these faults are shown in the figure 4.1 below.

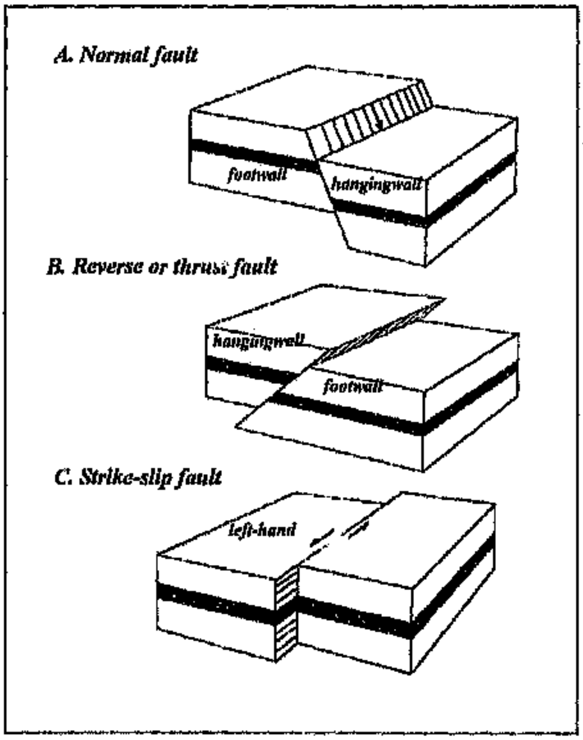


Figure 4.1. The geometric features of the three main types of faults (source: Ramsay & Huber, 1987).

These three types of faults seem to occur frequently in the natural fault systems and have been distinguished by Ramsay and Huber (1987) as follows:

Normal faults are inclined faults, usually with a dip exceeding about 50 degrees where the dip-slip component is large relative to the strike-slip component, and where the hangingwall is moved down relative to the footwall (figure 4.1a).

Strike-slip faults are those which are usually steeply oriented, often vertical with differential displacement between the walls that is predominantly horizontal (figure 4.1c).

Reverse faults are inclined faults, with inclinations generally less than 45 degrees, with a zero or small strike-slip component displacement and with a marked dip-slip component which give an elevation of the hangingwall relative to the footwall (figure 4.1b). Low angle reversed faults of this type (dip less than 45 degrees) are frequently termed thrusts or thrust faults. Because thrust faults are the dominant faults in the study area (Berlenbach, 1995), they are discussed in some detail. In thrust systems, the moved hangingwall block is termed a thrust sheet. Thrust complexes, made up of several thrust sheets, are sometimes bounded below by a well marked floor thrust, and may also be bounded by an uppermost roof thrust. Often a series of reverse faults branch from a floor thrust and produce a splay fault fan structure that is termed an imbricate structure. Such faults which splay off a common floor thrust, are called "ramps". In this structure, the strata are stacked like a reversed overlapping series of roof tiles. Imbricate fans, have been subdivided based on which of the subsidiary thrusts shows maximum displacement : where the maximum slip occurs on the frontal fault it is known as a leading imbricate fan (figure 4.2a), whereas an imbricated system where maximum slip occurs on the most internal fault is known as a trailing imbricate fan (figure 4.2b). Individual imbricate faults may terminate upwards, but often they curve asymptotically towards a common roof thrust so that the imbricate zone is contained between a roof and a floor thrust. Such a structure is termed a duplex (figure 4.2c). A more detailed description of the geometry, sequential initiation and development of these structures have been presented in Ramsay and Huber (1987).

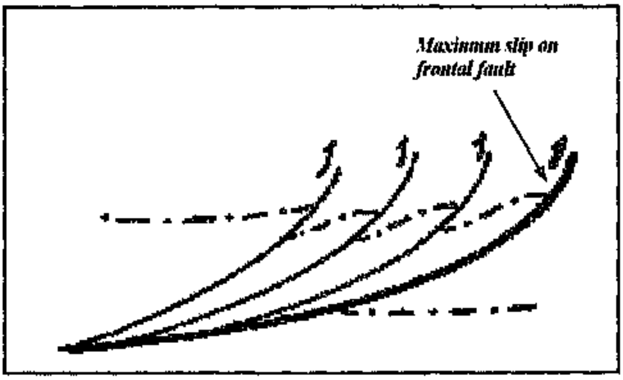


Figure 4.2a. Leading imbricate fan

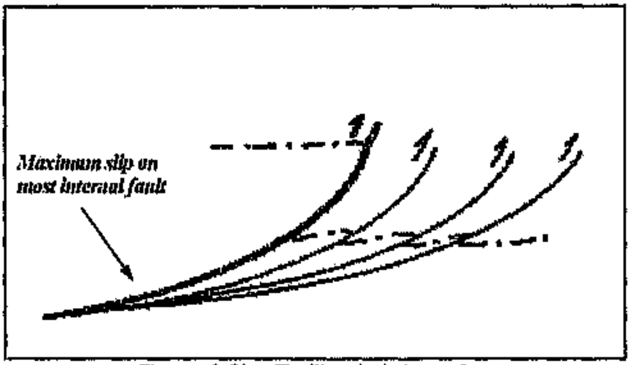


Figure 4.2b. Trailing imbricate fan

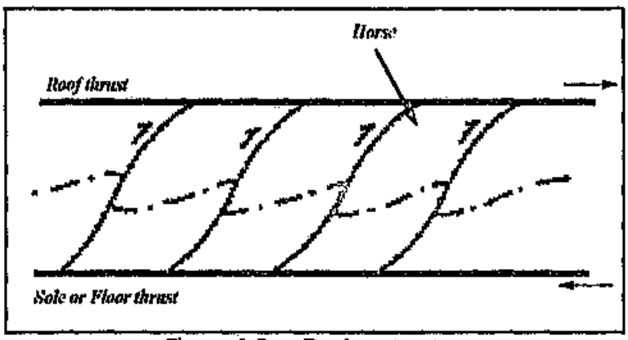


Figure 4.2c. Duplex structure

Figure 4.2. Terminology of thrust systems. Arrows indicate movement sense along fault planes.

## 4.3 Mapping

The objective of this study is aimed at improving support design by acquiring knowledge about the inclination, orientation and intensity of the mining induced fractures in relation to geological features. The method adopted for gathering data involved mapping the inclination and orientation of both, mining induced fractures and geological features like faults and joints. Basically, section lines were established along strike of the hangingwall, from the stope face up to about 30 m in the back area. Measurements were taken along this line with a Brunton compass and often checked with a clino-rule to ascertain the possible influence of magnetic substances on the readings. A magnetic declination of +20 degrees was later used to minimize deviation of the readings from the true north. The following were criteria used to differentiate between geological features and mining induced stress fractures: a fault is characterized by calcite or quartz veins, striations and slickensided surfaces. Mining induced stress fractures on the other hand were considered to represent clean discontinuities with little or no ride displacements and usually terminate abruptly on parting planes. Joints were distinguished from the mining induced fractures by their longer lengths of run cutting across other minor discontinuities and an infilling material like calcite or quartz, in their apertures.

### 4.3.1 Orientation analysis

The lower hemisphere projection technique embedded in the DIPS computer programme was used to plot and analyze the data. Details about the method have been outlined in Hoek and Brown (1980). This has been summarized in figure 4.3.

Fig. 4.3a shows an imaginary plane cutting across a reference sphere. The intersection of this plane and the surface of the sphere designated by the shaded region, is a great circle. If a line is assumed to be run through the center of the sphere in a direction perpendicular to this plane, it will pierce the sphere at two diametrically opposite points which are called poles of the great circ' epresenting the plane. For the lower hemisphere projection, only the pole in the lower half of the sphere is considered. This pole can further be projected on the horizontal plane of the lower reference hemisphere as shown in figure 4.3b. The results of these projections are shown in figure 4.3c.

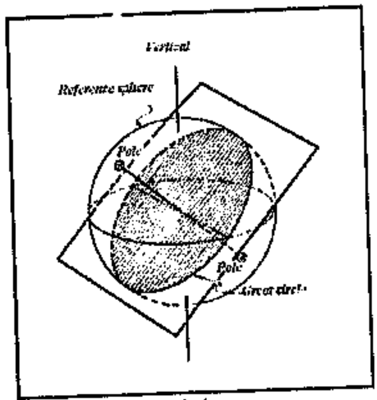


(a)

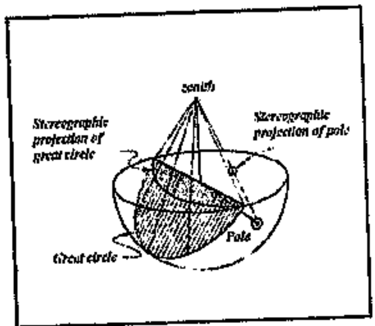


(b)

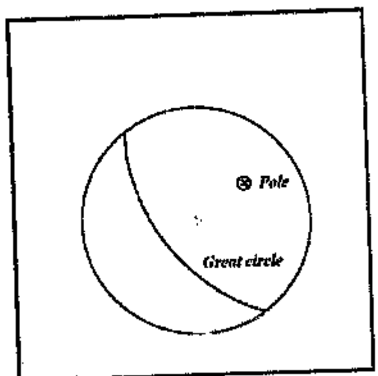


(c)

Figure 4.3. Figure 4.3a shows a great circle and its poles. These define the inclination and orientation of a plane. Figure 4.3b illustrates the stereographic projection of the great circle and its pole onto the horizontal plane of the lower reference hemisphere. Figure 4.3c shows final result of the stereographic projection.

4.3.2 **Presentation of results**

The observations made in each of the two stopes are presented separately in the following subsections (see mine plans in figures 3.5 and 3.6).

4.3.2.1 Observations in north panels

Observations made in this panel revealed that thrust faults in the hangingwall seem to be the main geological structures traversing the area. Generally these are low dipping faults. Their surfaces are slickensided with the striations orientated towards the north-eastward direction. Quartz veins are common features. These give an indication that there is a bedding parallel fault at the contact between the VCR and the soft lava along which movement has taken place (figure 4.4).

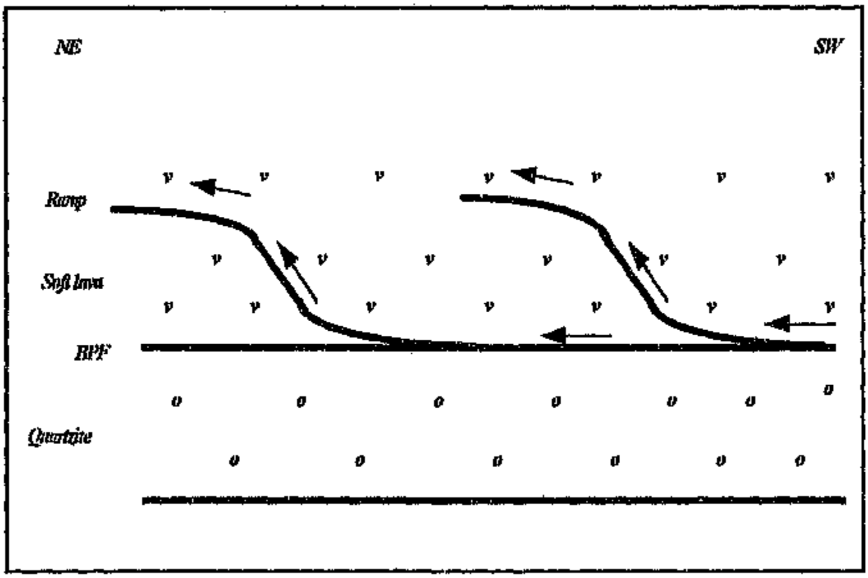


Figure 4.4. Simplified geometry of the imbricate system in the study area, bedding-parallel faults along the VCR/soft lava contact step up into the hangingwall along steeper dipping ramps. Arrows indicate movement directions (modified after Berlenbach, 1995).

This plane can be regarded as a floor thrust. The low dipping thrust faults that appear to branch off from the main floor thrust into the soft lava represent an imbricate structure. These structures were observed to occur along strike. Their point of inflexion was however not conspicuous. There seems to be a recurrence of these structures at intervals of between 5 - 8 m along strike. On all occasions, their first occurrence was noticed at about 10 - 15 m from the stope face. The hangingwall within this interval was virtually smooth. As the span increases, a fall of ground usually occurs which then exposes this structure. A typical distance of the area exposed stretches over about 13 m along dip and about 190 cm into the hangingwall. Figure 4.5 is a simplified section, indicating the complex relationship between these faults and the mining induced fractures. These observations are substantiated by the attached photographs i.e. figures 4.6 and 4.7.

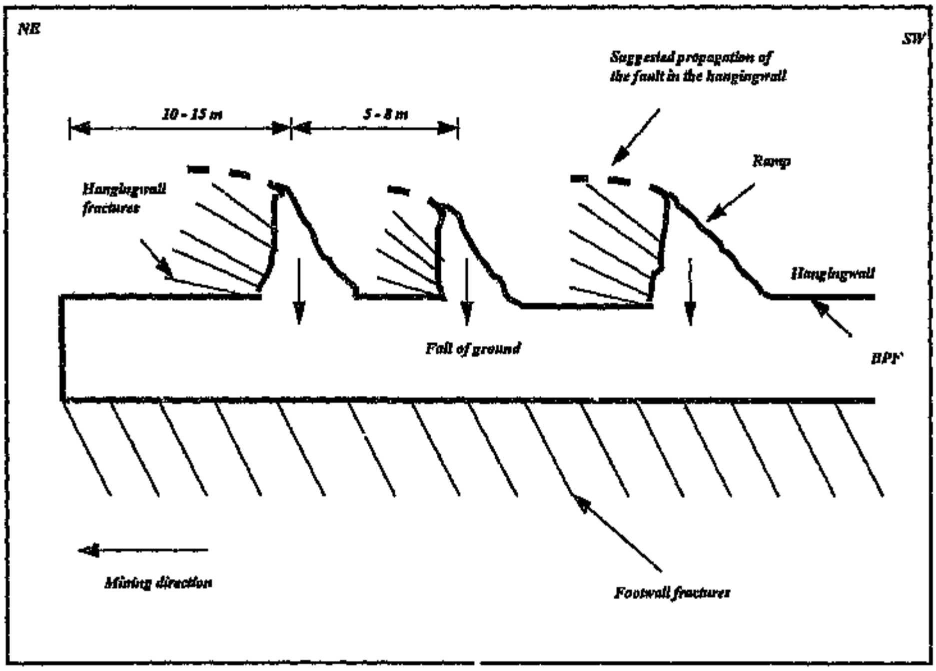


Figure 4.5 A simplified strike section show the complex relationship between mining induced stress fractures ...gical structures in the north panels.

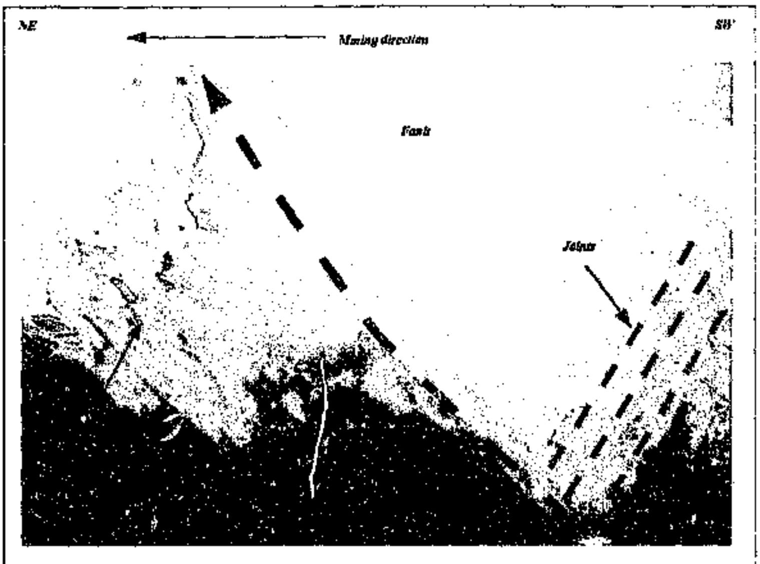


*The dashed arrow indicates the direction of movement along the fault.*

Figure 4.6. The orientation of mining induced stress fractures in the vicinity of geological structures in north 2 panel.

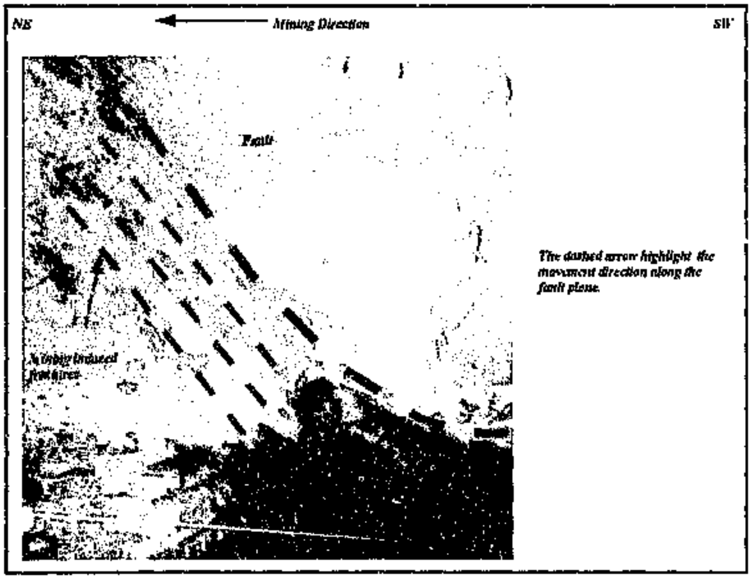


Figure 4.7. An illustration of the movement direction along a thrust fault in north 2 panel.

#### 4.3.2.1.1 Stereographic projection of features in the north panels

The lower hemisphere projection technique has been used to analyze the data gathered. The results have been presented in three separate diagrams in figure 4.8. The numbers on these figures help to identify a pole and its corresponding plane. In all the three cases pole concentrations specifying the orientation of the structures have been contoured. The mean orientation of structures has been deduced from the point of maximum pole concentration. Corresponding major planes have been drawn. In figure 4.8a, the faults strike approximately face-parallel and dip towards the back area. From underground observations mining induced stress fractures tend to cluster around the faults and assume a similar orientation to the thrust faults, see figure 4.8b. In contrast, the joints appear to be dipping towards the stope face but strike approximately face-parallel as shown in figure 4.8c. Figure 4.9 shows the unfavourable intersection of these structures which leads to the isolation of unstable 'traingular' blocks in the hangingwall.

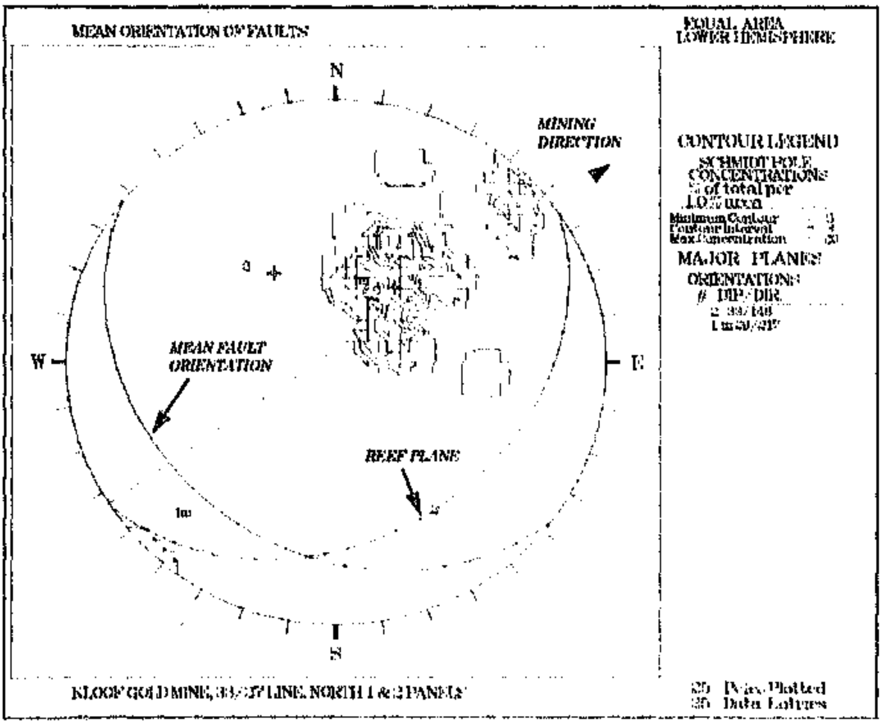


Figure 4.8a. Orientation of faults in the north panels.

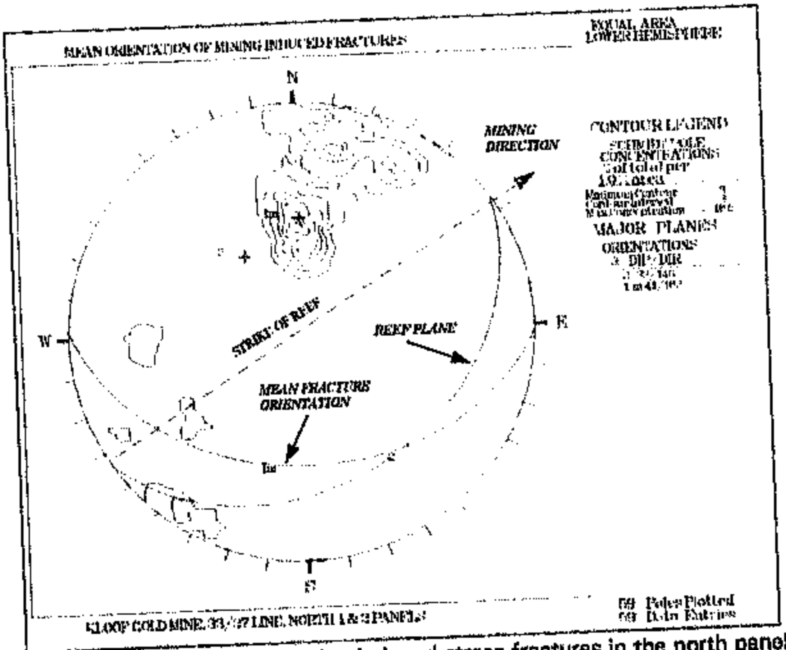


Figure 4.8b. Orientation of mining induced stress fractures in the north panels.

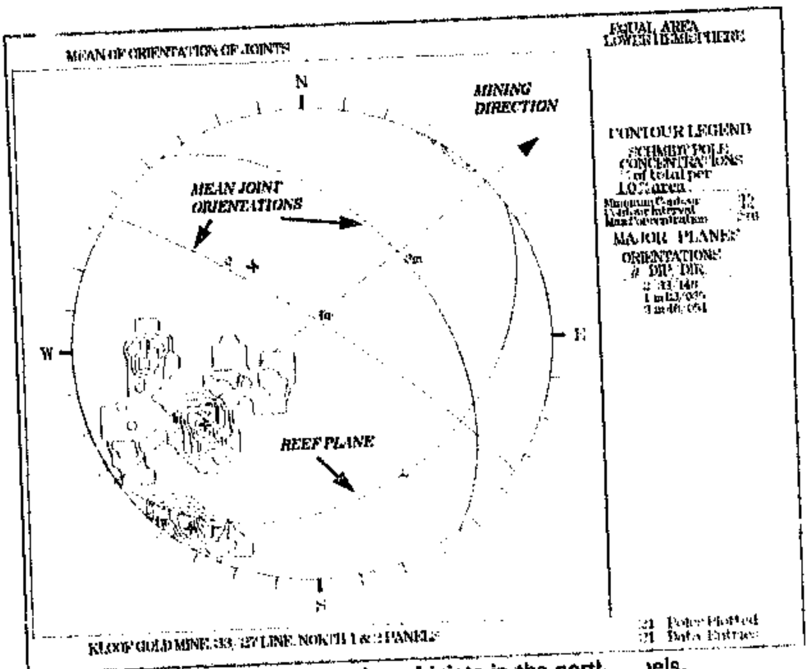


Figure 4.8c. Orientation of joints in the north panels.

## Interpretation

The orientations of joints, faults and mining induced fractures have been presented separately in each of the in the above diagrams. The major planes representing each of the above projections have been presented in figure 4.9 below. The stippled region demarcates an area bounded by these three structures in the hangingwall. This represents the typical shape of an isolated piece of rock that may be formed by the unfavourable intersection of geological structures and mining induced fractures. This accounts for the fall of ground patterns observed between the timber packs as stated earlier. Thus the orientation and inclination of these structures affects the stability of the hangingwall.

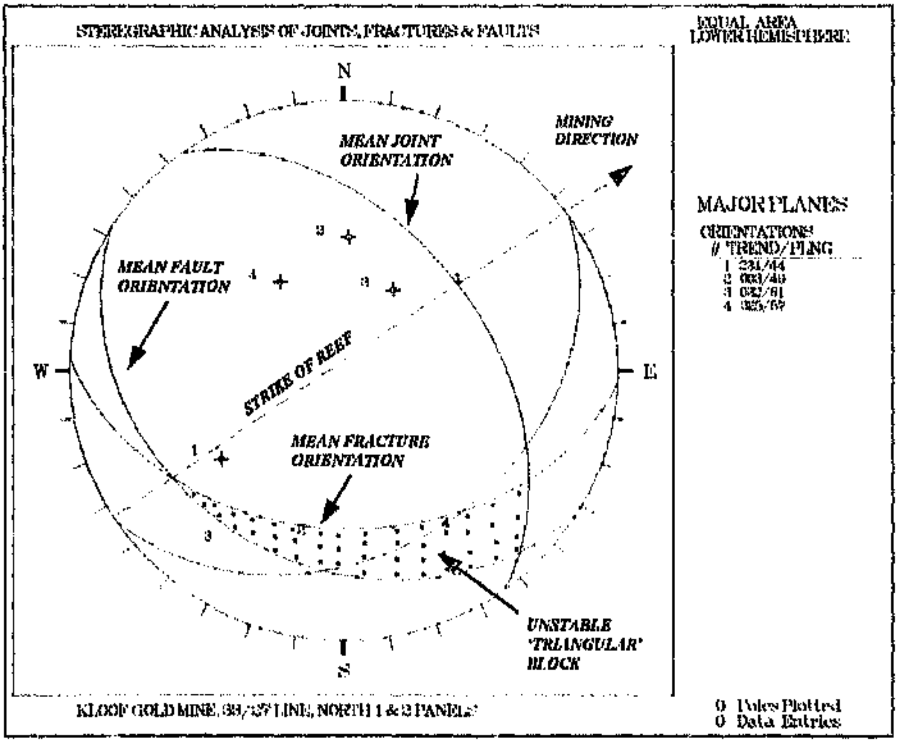


Figure 4.9. Intersection of joints, faults and mining induced stress fractures.

#### 4.3.2.2 Observations in south 1 panel

Geological features particularly the thrust faults described above, lacked exposure in the southern stopes. However, there was some evidence that they do exist. The few that were exposed and could easily be identified had similar features (i.e. striations, slickensides and the calcite or quartz veins) like those noted in the north panels. A characteristic feature that is believed to affect the stability of the hangingwall is a bedded quartzite layer that is quite common between the VCR and the Soft lava. The average spacing between successive beds is 130 mm.

Mining was being advanced on strike towards the south-west. The mining induced fractures dip steeply towards the face. Underground observations showed that they strike approximately parallel to the stope face. Unstable keyblocks were bounded by fractures dipping at various angles to the mining direction. An illustration of a strike section across the stope depicting the orientation of the fractures and probable thrust faults in the hangingwall is shown in figure 4.10 below. Some underground photographs are shown in figures 4.11 and 4.12.

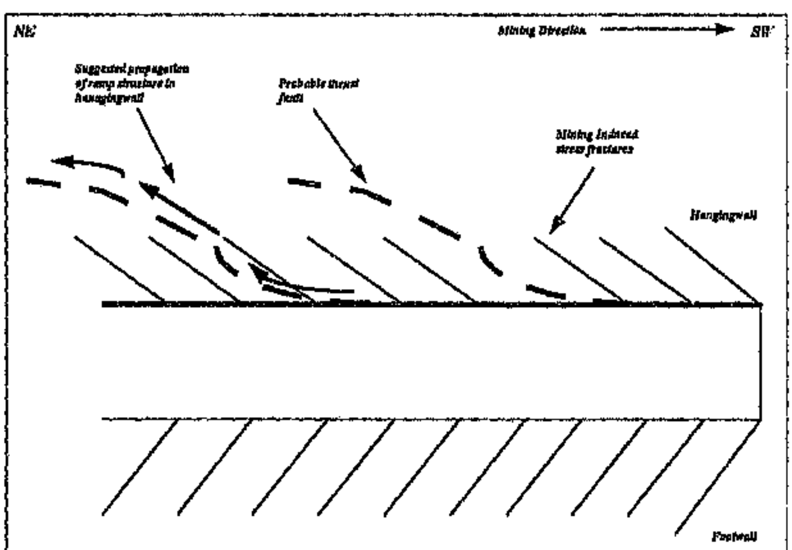


Figure 4.10. A simplified strike section showing the orientation of mining induced stress fractures and probable thrust faults in the south panels.

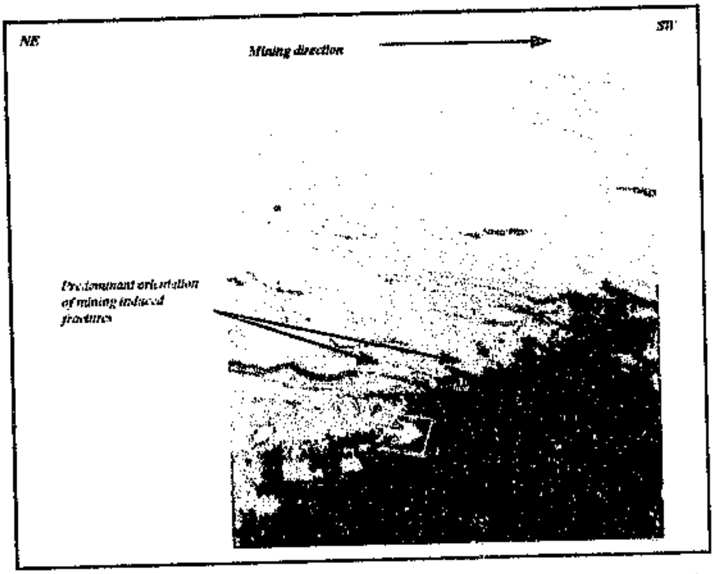


Figure 4.11. General orientation of mining induced stress fractures in the south panels.

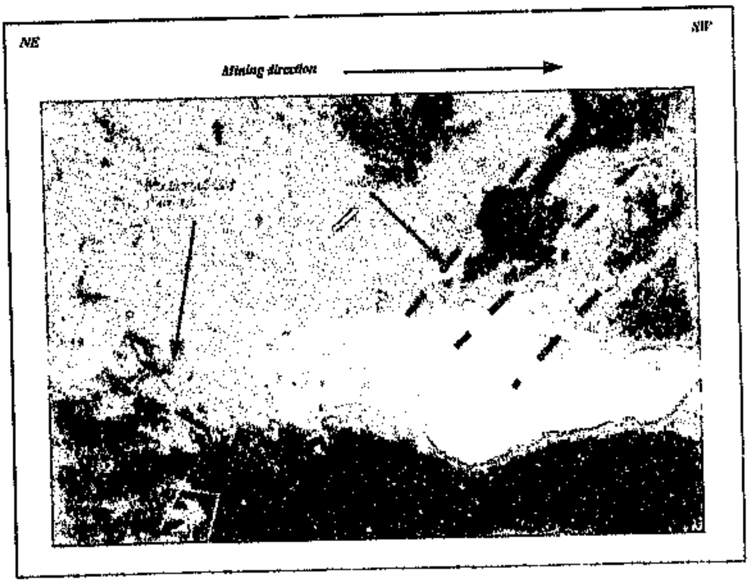


Figure 4.12. Unfavourable intersection of mining induced stress fractures and joints in south 1 panel.

#### 4.3.2.2.1 Stereographic projection of data collected in South 1 panel

Figure 4.13 shows the results of the stereographic projection of mining induced stress fractures. The line running through the diameter of the great circle designates the strike of the reef and also indicates the direction of mining i.e. towards the south-west. The orientation of the reef has been represented as a major plane dipping towards the south-east. Contours of the poles representing the orientation of the mining induced stress fractures have been drawn. The contour plot displays two distinct concentrations of fractures. The first group are steeply dipping and approximately face parallel. The second group of fractures are less steeply dipping and strike obliquely to the face. The last group represent shallow dipping fractures and strike in an approximately perpendicular to the face. Major planes corresponding to each of these concentrations have been drawn as shown in figure 4.13. The pole concentrations of the geological features do not feature prominently on the diagram due to their inconspicuous nature during the measurements.

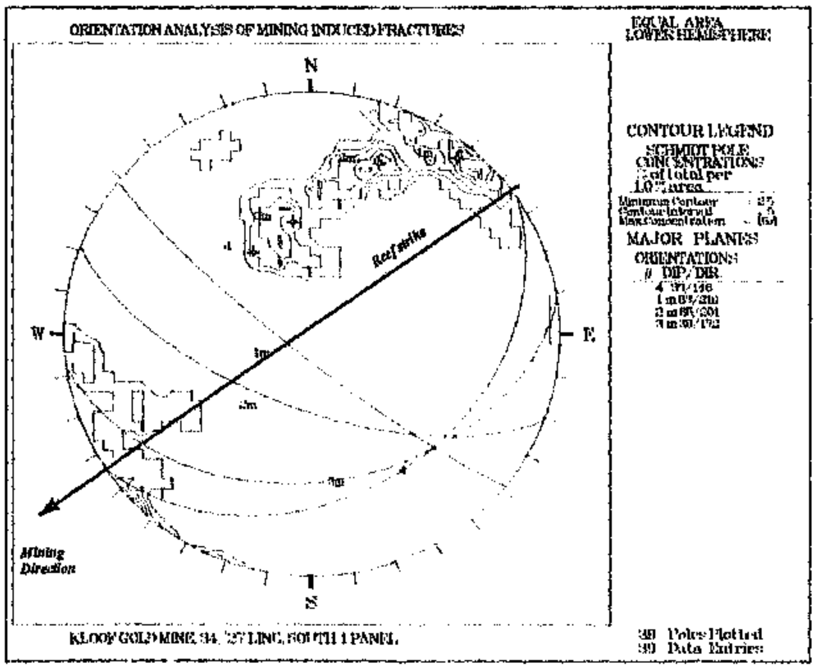


Figure 4.13. Stereographic projection of mining induced stress fractures in south 1 panel.

# CHAPTER FIVE

## NUMERICAL MODELLING

### 5.1 Introduction

One of the main aims of this project is to develop a conceptual model for the rock mass behaviour around VCR stopes. This objective is aimed at providing some framework for the design of stope support. In the different VCR geotechnical areas, different behaviour of the rock mass surrounding the VCR have been observed. It was suggested that these differences might be due largely to the different rock properties that character' various rock types in these areas. In addition, geological features such as bedding .l faults and joints appear to influence the behaviour of the rock mass. An essential part of the conceptual model is an understanding of the factors that result in the changes in behaviour.

The computer program FLAC has been used to model the multi-material rock mass surrounding a stope. FLAC is a two-dimensional explicit finite difference code. In the finite difference method (FDM), the body is represented as a continuous solid for the purposes of the analysis. Materials are represented by elements, or zones, which form a grid that is adjusted to fit the shape of the object to be modelled. Cundall (1986) explains that each element behaves according to a prescribed linear or non-linear stress/strain law in response to the applied forces or boundary restraints. If the stresses are high enough to cause the material to yield and flow, the grid can actually deform (in large-strain model and move with the material that is represented. The displacements, velocities and accelerations are calculated at discrete grid points. The displacement field is computed by approximating the differential equations for the system as a set of difference equations that can be solved discretely at each grid point. The programming language embedded in FLAC i.e. FISH has been used to define various functions. These functions enable the excavation sequence to be controlled and to store, analyze and plot the fracture angles formed during the excavation process.

Two constitutive material models i.e. Mohr-Coulomb and Mohr-Coulomb with strain softening and associated properties have been assigned to all zones in the model. Laboratory testing of rock samples has been performed to provide input parameters to be used in the model. The model was initially developed by Dr. Robin Eve of CSIR, Miningtek for analysis with FLAC. The model has been adapted and applied to simulate the rock mass behaviour at the geotechnical area on Kloof Gold Mine. It has further been extended to look at the performance of three back area support types. It must be emphasized that the models are highly simplified representations of the physical reality. The present work has served to identify some of the limitations of the models in terms of predicting the orientation of extension fractures formation. Consequently, although the scope of the modelling work is currently rather modest the preliminary stages of the work are described and a recommendation is made for further studies to provide greater insights into fracture formation.

## 5.2 Model geometry

The model represents the excavation of a stope with a mining height of 1.4 m. Vertical symmetry at the center of the stope is used and a 40 m half span is allowable. To represent the rock mass surrounding the stope, boundaries are placed at 90 m above and below the stope and 140 m ahead of the final stope face position. Bedding planes at a spacing of 0.5 m have been defined to a distance of 5 m below the stope, this is to simulate the bedded rock types like quartzite encountered in reality. The grid geometry is illustrated in figure 5.1.

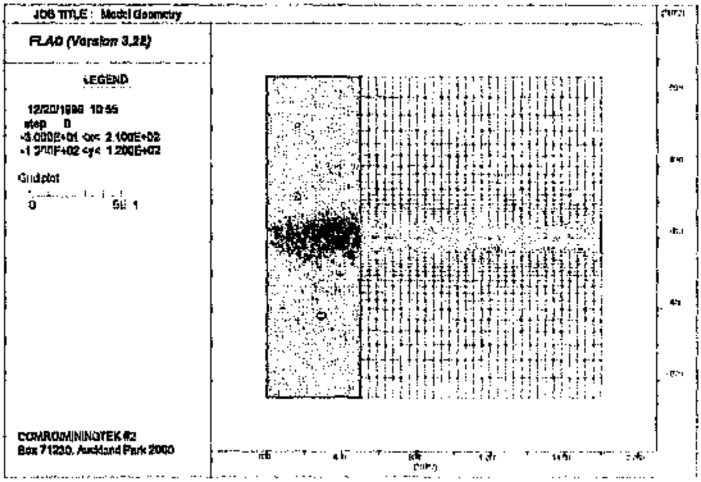


Figure 5.1. Grid Geometry.

## 5.3 Boundary and initial conditions

The modelling has been restricted to considering a single horizontal stope in a finite rock mass, the influence of any other mining is ignored. The boundary and initial conditions are used to include the influence of depth and the confining influence of the rock on the model. The stope that is considered is at a depth of 2755 m, where in-situ stresses of 74.3 MPa in the vertical, y, direction and 37.2 MPa in the horizontal, x, direction (k ratio = 0.5) may apply. These are typical of those that would be acting in virgin rock on a South African gold mine. The effects of gravity are included in the model, the virgin stresses, therefore, vary vertically over the model region. Initial stresses that take into account these variations and maintain the k-ratio are applied over the full domain. A symmetry condition is applied on the left-hand side of the model by simply stopping the boundary from moving in the horizontal, x, direction and ensuring that there is no shear stress. The bottom and top boundaries have been fixed in the y direction. Stresses are applied to the right hand side of the model (see figure 5.2). The stresses within the model have been initialized to virgin stress levels. The model is initially stepped to equilibrium through a few cycles. This helps to reduce the solution time.

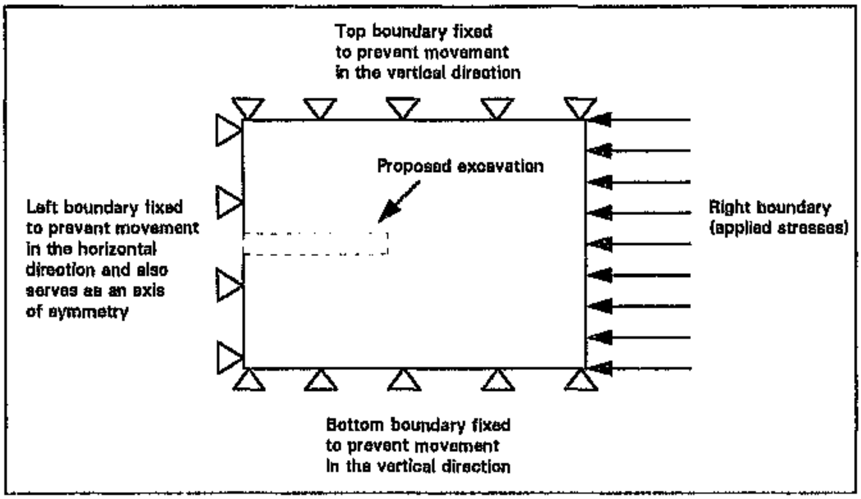


Figure 5.2. Schematic representation of boundary conditions.

## 5.4 Mining

As mining progresses, stresses are induced in the rock mass surrounding the excavation. Consequently the resultant stress acting on the rock mass increases. This stress change contributes largely to the observed deformation characteristics of the rock mass. Principal stress directions are taken to be an indication of the direction at which fractures form; extension fractures are assumed to form parallel to the direction of major principal stress. A FISH function is used to record the direction of the principal stress in the FLAC grids just ahead of the face. This information is stored in such a way that it may be plotted as lines that depict the hypothesized fracture direction. Plots of these angles in the first grid in the hanging and footwall versus stope span can be obtained. The constitutive model is not adjusted for the presence of fractures. The Mohr-Coulomb failure criterion is used to determine when fractures are formed. The fracture directions recorded in this way are compared with those observed underground. A FISH function has also been incorporated to calculate and plot the amount of relative displacement between the hangingwall and footwall versus face advance at specified points along the skin of the excavation. A total number of 80 face advance steps of 0.5 m are modelled to give a final stope half span of 40 m. The FISH utility 'ZONK' is used to ensure stability of the excavation. This is achieved by extracting a given region of zones and gradually, relaxing the forces existing around the newly mined region. The effects of blasting in mining have not been incorporated into the model. The material surrounding the excavation is assumed to be stable during mining.

## 5.5 Material properties

The problem domain has been represented as a series of discrete gridpoints, these define zones to which different material properties can be assigned. The zoning has been made as fine as possible near the stope and coarser towards the boundaries; the transition between coarse and fine zoning is as smooth as possible. This gives better accuracy in the area of interest, near the stope, while reducing the size of the problem. Rock samples were collected from the study site and tested in the laboratory to provide input parameters for the model.

### 5.5.1 Laboratory rock testing

The general response of the rock mass to the varying degrees of stress imposed on it by mining is highly controlled by its inherent properties. One of the main strategies adopted to improve the understanding of the rock mass behaviour surrounding the VCR was to develop a conceptual model. A good conceptual model requires good input data, hence the need to determine the strength characteristics of the hangingwall and footwall rock types in this geotechnical area.

Hangingwall and footwall rock samples were collected from this geotechnical area. Core samples measuring 76.2 mm in length and 25.2 mm in diameter were prepared. Triaxial tests were carried out at 10 MPa, 20 MPa, and 40 MPa confinements in a stiff machine and the post failure behaviour of the samples were recorded. Each of these suite of tests were conducted in each of three directions i.e. dip, strike and 90° relative to the reef plane so as to ascertain whether the rocks exhibit any anisotropy. However, no significant differences between the different directions were noted. The results obtained for the soft lava and quartzite are presented in figures 5.3 and 5.4 respectively below.

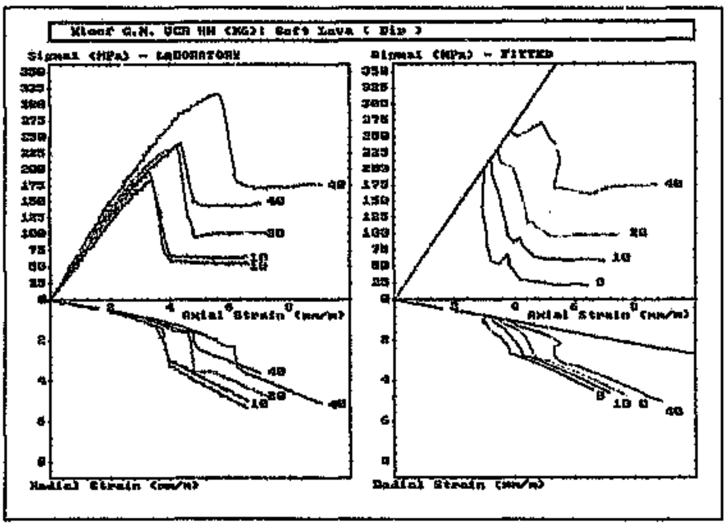

Figure 5.3a. Laboratory tests results for soft lava showing graphs of major principal stress and radial strain against axial strain at different confining stresses.

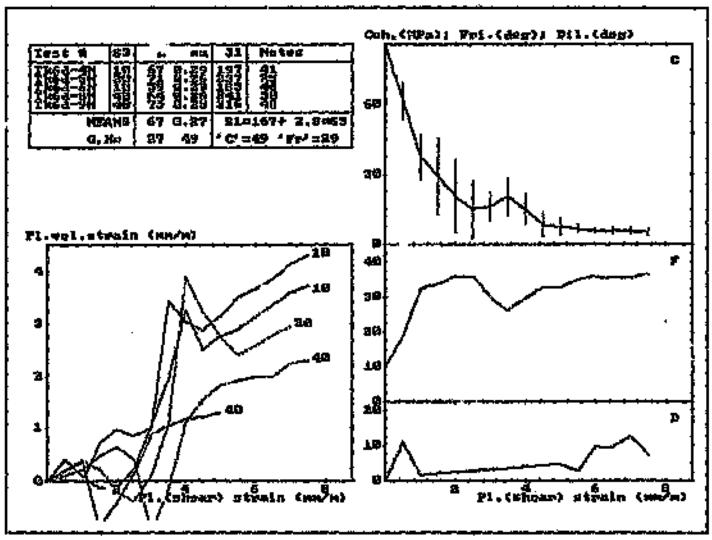

Figure 5.3b. Laboratory tests results for soft lava showing graphs of cohesion, angle of internal friction and dilation against shear strain.

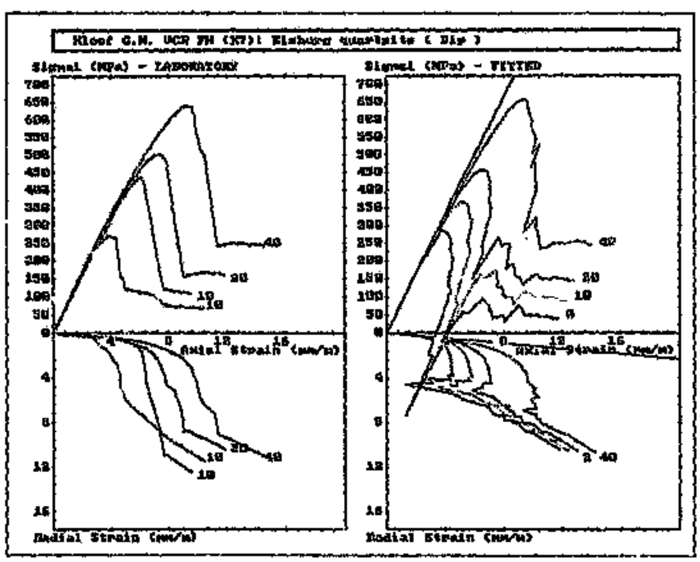

Figure 5.4a. Laboratory tests results for quartzite showing graphs of major principal stress and radial strain against axial strain at different confining stresses.

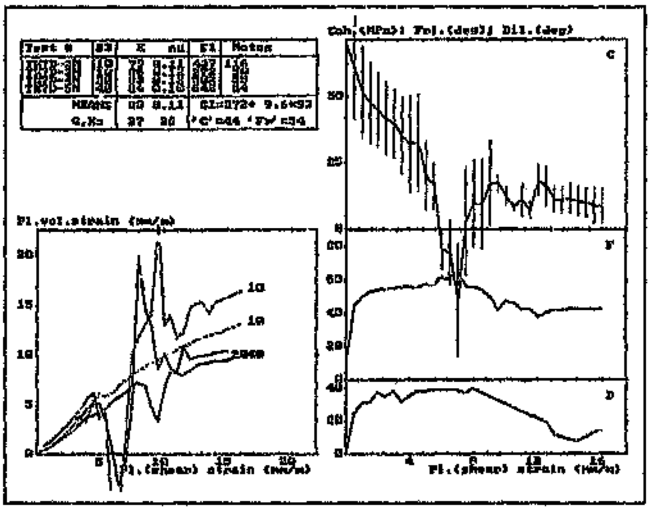

Figure 5.4b. Laboratory tests results for quartzite showing graphs of cohesion, angle of internal friction and dilation against shear strain.

The SS VisualBasic programme written by John Ryder was used to interpret the parameters required by the strain-softening model that is embedded in FLAC, in terms of more familiar triaxial stress-strain characteristics. The results are presented in figures 5.5a and 5.5b below.

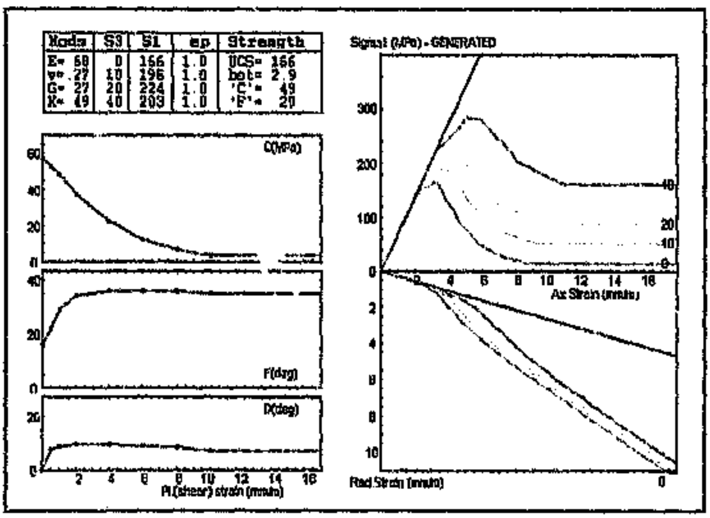


Figure 5.5a. Strength characteristics of soft lava obtained from SS programme.

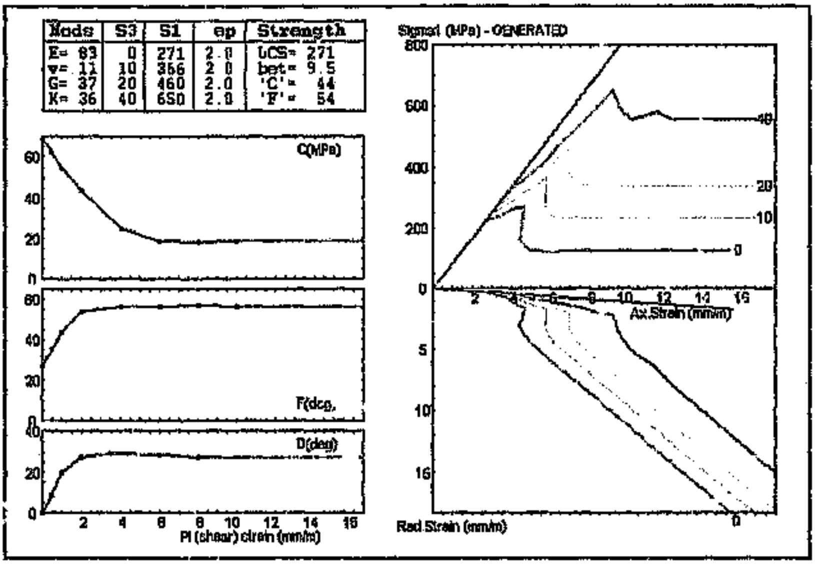


Figure 5.5b. Strength characteristics of Elsburg quartzite obtained from SS programme.

It is noted that precise rock properties for the reef have not been measured; the coarse pebbly structure of the reef cannot reliably be tested using the standard triaxial tests used to obtain the properties of hangingwall and footwall rock types. Properties of quartzite material have been used, a softer or at least more rapidly softening behaviour may be more appropriate as crushing of the stope plays an important role in determining the stress distribution from which the fracture angles are being inferred. Two constitutive models available in FLAC have been used to investigate which model best represents the rock mass behaviour at the geotechnical area on Kloof Gold Mine. These are Mohr-Coulomb and Mohr-Coulomb with strain softening models. The Mohr-Coulomb with strain-softening model proved most successful. The laboratory rock testing results provided input parameters for these models.

### 5.5.2 Mohr-Coulomb model

The Mohr-Coulomb plasticity model represents a material that can yield in shear; in FLAC this model also includes a tension limit criterion. The basic parameters in Mohr-Coulomb plasticity are defined as density $\rho$, bulk modulus K, shear modulus S, tension cut-off T, dilation angle $\psi$, internal friction angle $\phi$, and cohesion C.

**Representation of VCR rock mass using Mohr-Coulomb model**

The Mohr-Coulomb model has been applied to represent the rock mass at the study site. The material properties assigned to the model are listed in table 5.1. The actual laboratory results for the cohesion and internal friction angle have been degraded by 50%. The tension cut-off represents 10% of the resulting cohesion value. These values were arrived at after series of iterations to establish realistic degrading values that conform to underground observations.

The results of Mohr-Coulomb model indicated that the stress around the stope changes depending on internal friction angle $\phi$, the dilation angle $\psi$, the tension cut-off T, and-the cohesion C. Large differences in cohesion appear to be the most significant.

Table 5.1. Material properties used in the Mohr-Coulomb model

| PROPERTY | KLOOF | |
|---|---|---|
| | Hangingwall soft lava | Footwall quartzite |
| density (kg/m $^3$) | 3e3 | 3e3 |
| Bulk Modulus K (GPa) | 49 | 35.6 |
| Shear Modulus G (GPa) | 27 | 37.2 |
| Cohesion C (MPa) | 28 | 22 |
| Internal friction angle (degree) | 14.5 | 27 |
| Tension cut off T (MPa) | 2.8 | 2.2 |
| Dilation angle $\psi$(degree) | 7.6 | 8.8 |

### 5.5.3 Strain-softening model

The strain softening model implemented is a plasticity model based on the Mohr-Coulomb constitutive model. The principal characteristic is that the strain softening model incorporates load shedding upon loading beyond peak strength. In addition to the two elastic constants, Young's Modulus E and Poisson's ratio v, the strain softening model requires the specification of cohesion C, internal friction angle $\phi$, and dilation angle $\psi$ as a function of plastic strain as depicted in figures 5.5a and 5.5b above.

**Representation of VCR rock mass behaviour using strain softening model**

In addition to the Mohr-Coulomb properties listed above, the material properties assigned to the strain softenin model are specified in table 5.2. The actual laboratory results for the cohesion and internal friction angle have degraded by 50% to account for the inhomogeneous nature of the in-situ rockmass.

Table 5.2. Material properties used in the strain softening model

| Cohesion | | | | Friction | | | | Dilation | | | |
|---|---|---|---|---|---|---|---|---|---|---|---|
| Hangingwall | | Footwall | | Hangingwall | | Footwall | | Hangingwall | | Footwall | |
| mm/m | MPa | mm/m | MPa | mm/m | deg | mm/m | deg | mm/m | deg | mm/m | deg |
| 0,0 | 28,6 | 0.0 | 34,5 | 0,0 | 8.2 | 0,0 | 14 | 0.0 | 0.0 | 0.0 | 0.0 |
| 0,5 | 26,5 | 0,5 | 31.0 | 0.5 | 11.0 | 1.0 | 22 | 0.5 | 7,6 | 0.5 | 8.8 |
| 1,0 | 24.4 | 1,0 | 27.5 | 1,0 | 14,6 | 2.0 | 27 | 1,0 | 8.6 | 1.0 | 20.0 |
| 2.0 | 18.6 | 2.0 | 22.0 | 2.0 | 17.0 | 4.0 | 28 | 2.0 | 9.6 | 2.0 | 27.6 |
| 4.0 | 11.4 | 4.0 | 12.5 | 4.0 | 18.0 | 6.0 | 28 | 4.0 | 9.6 | 3.5 | 29,6 |
| 5.0 | 6,4 | 6.0 | 9,50 | 6.0 | 18,0 | 8,0 | 28 | 6,0 | 8.5 | 6.0 | 28,8 |
| 8,0 | 3,5 | 8.0 | 9.00 | 8.0 | 16.0 | 10.0 | 28 | 8.0 | 8.2 | 8.0 | 27.2 |
| 10.0 | 2.0 | 10,0 | 9,60 | 1.0 | 17.4 | | | 10.0 | 7,2 | | |

**Results**

The development of plastic failure area occurs a few zones ahead, below ar above the stope. The results indicated that large differences in cohesion appear to be more significant than differences in the other plasticity parameters, internal friction angle $\phi$ and dilation $\psi$. The stress distribution around the stope and the orientation of the major principal stress obtained by using the model are shown in figures 5.6a and 5.6b respectively. It is assumed that the orientation of the fractures would form parallel to the direction of the major principal stress. The fractures in the hangingwall would then be almost vertical whereas the fractures in the footwall would be steep and dip away from the face. This pattern is similar to what was observed during underground visits, particularly in the south panels (see figure 4.10 above).

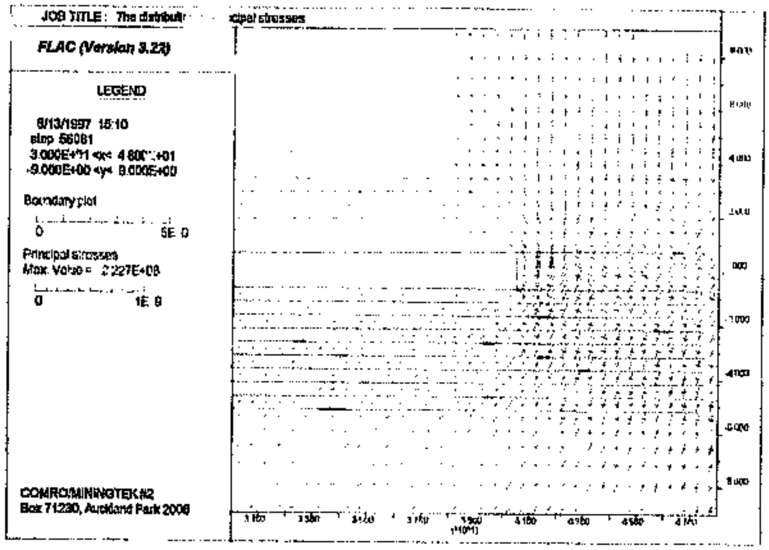

Figure 5.6a. Distribution of principal stresses obtained by using the Mohr-Coulomb model to represent the rock mass at Kloof Gold Mine.

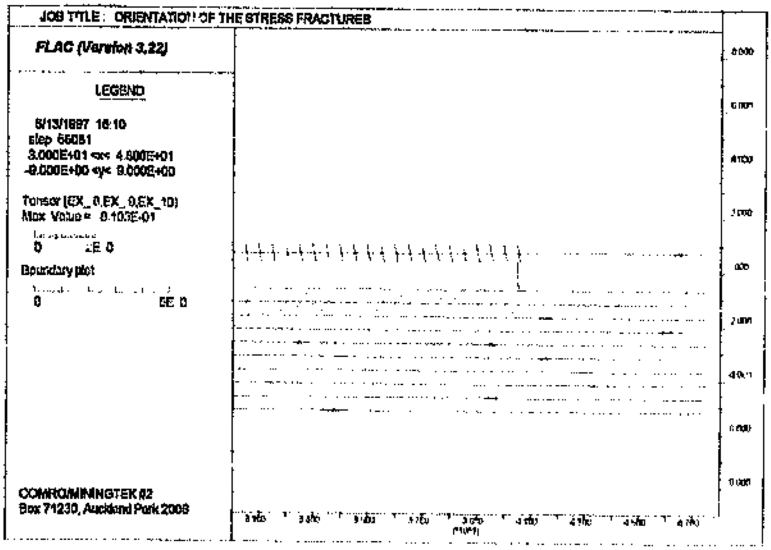

Figure 5.6b. Inferred direction of fracturing around the excavation obtained by using the Mohr-Coulomb model to represent the rock mass at Kloof Gold Mine. Ex_8, Ex_9 and Ex_10 are extra grid variables that represent fictitious Sxx, Syy and Sxy components of the fracture tensor respectively.

Limitations

There are a number of limitations inherent to the approach described above. One criticism is that the inelastic constitutive laws used account only for plasticity associated with shearing while the fracture patterns being evaluated are extensional. This remains unanswered. There are also some limitations to the way in which results have been interpreted. In the work described above principal stress directions have been taken to be an indication of the direction at which fractures form; extension fractures are assumed to form parallel to the direction of major principal stress.

While the fracture directions recorded compare reasonably well with those observed underground, on closer inspection of a principal stress plot around the face of an excavation, it can be seen that there are reasonably large differences in the magnitude of the principal stresses in zones ahead of the face. This suggests that fracturing may not occur at the same distance from the face in the hangingwall and footwall. To improve the current interpretation of results some method of determining when to record the formation of a fracture is necessary. Currently, the constitutive model is not able to adjust for the presence of fractures, such an adjustment would improve results.

### 5.5.4 Extension of the model

The model has been extended to include Mohr-Coulomb with strain-softening and ubiquitous joint models for the rock mass behaviour at the study site. The objective of this extension was to look at the performance of back area support in this geotechnical area. The region extending up to about 10 m above the stope is assigned ubiquitous joint properties. This preserves preferential slip directions determined by failure ahead of the face in the hangingwall when the face advances and the stresses acting change orientation. The angle of the ubiquitous joints has been varied to reflect the observations made underground. The remaining hangingwall and footwall are given Mohr-Coulomb properties. The material properties are given in table 5.3.

**Support**

As mining progre' .es, interfaces are inserted by defining the interacting gridpoints at the skin of the hangingwall and footwall. Support units are then installed at 3 m center-to-center intervals. The performance of three back area support types namely solid matpacks, profile prop unturned and classified tailings (48% porosity) have been analyzed. The performance curves for these support types downgraded by 25% for underground installation are shown in figures 5.7, 5.8 and 5.9 below.

Table 5.3. Material properties used in Mohr-Coulomb and Ubiquitous joint models for the rock mass at Kloof Gold Mine.

| Properties | Hangingwall (Soft lava) | Footwall (quartzite) |
|---|---|---|
| Density | 3e3 | 3e3 |
| bulk modulus(GPa) | 49.0 | 35.6 |
| shear modulus (GPa) | 27.0 | 37.2 |
| cohesion (MPa) | 27.8 | 22.0 |
| friction angle (deg) | 14.5 | 27.3 |
| dilation (deg) | 8.6 | 8.8 |
| tension cut-off (MPa) | 2.8 | 2.2 |
| joint friction angle (deg) | 10.9 | |
| joint cohesion (Mpa) | 20.9 | |
| joint angle (deg) | 105 | |
| joint tension (MPa) | 2.1 | |

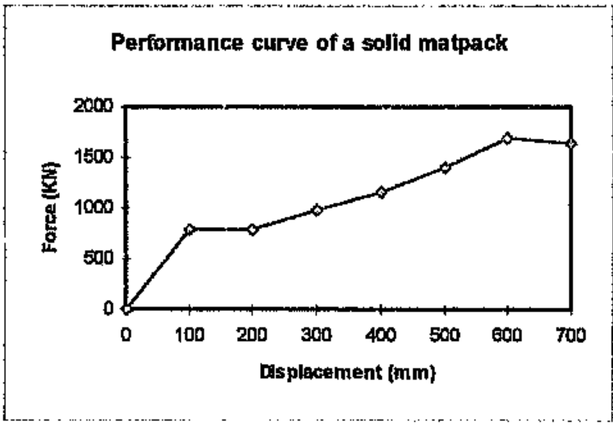


Figure 5.7. Performance curve of solid matpack.

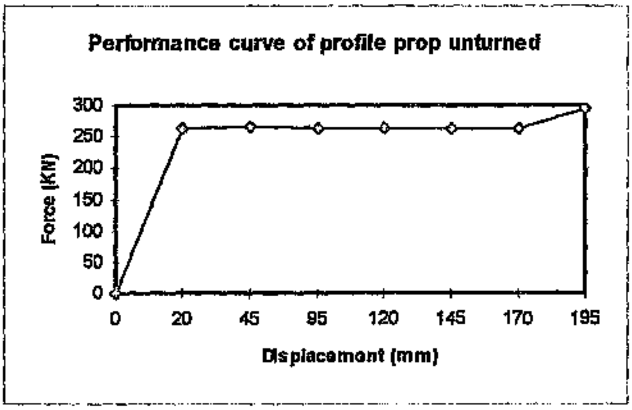


Figure 5.8. Performance curve of profile prop.

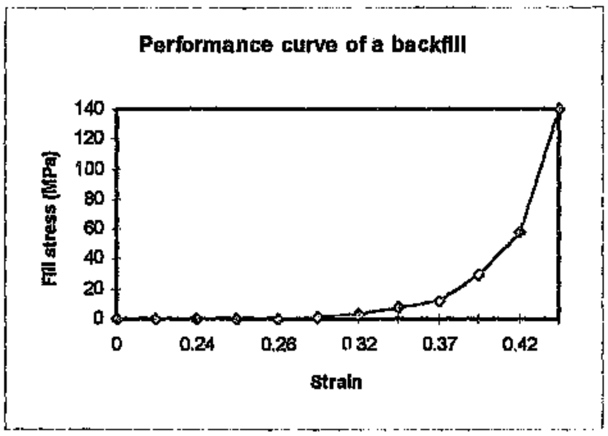


Figure 5.9. Performance curve of backfill (classified tailing).

**Results**

Some of the results obtained for the rock mass at Kloof Gold Mine are shown in figures 5.10 and 5.11. Figure 5.10 shows the representation of the rock mass using solid matpack as back area support. The state flags produced by the FLAC solution give an indication about the extent of failure around the excavation. The ubiquitous joint angle was set at 105 degrees in this model. Slip along the joint surfaces has also been indicated. The amount of relative displacement between the hangingwall and footwall was monitored at 25 m behind the stope face and the results have been plotted in figure 5.11. Figure 5.11a shows the rate of closure when no support is installed. Figures 5.11b and 5.11c show that matpacks and profile props, respectively, start building up resistance to closure soon after installation. The backfill appears to have little initial influence on closure rate until the face position reaches 10 m from the monitoring point (see figure 5.11d). This is partly because of the lower initial stiffness of backfill. Therefore the model has been tested for a 80 m half span. This involved placing the boundaries at 140 m above and below the stope and 200 m ahead of the final stope position. The input parameters used in the 80 m half span model are the actual laboratory results without any downgrading. This is because initial runs made with the same material properties as specified in the 40 m half span model resulted in unreasonably high deformations. The convergence was monitored at 55 m behind the final stope face. The results obtained are shown in figures 5.12a to 5.12d. Figure 5.12d shows that the performance of the backfill is better than that of the props and packs. While the backfill stabilized the convergence to about 170 mm, the props and packs minimized the it to 220 mm and 270 mm in see figures 5.12b and 5.12c respectively.

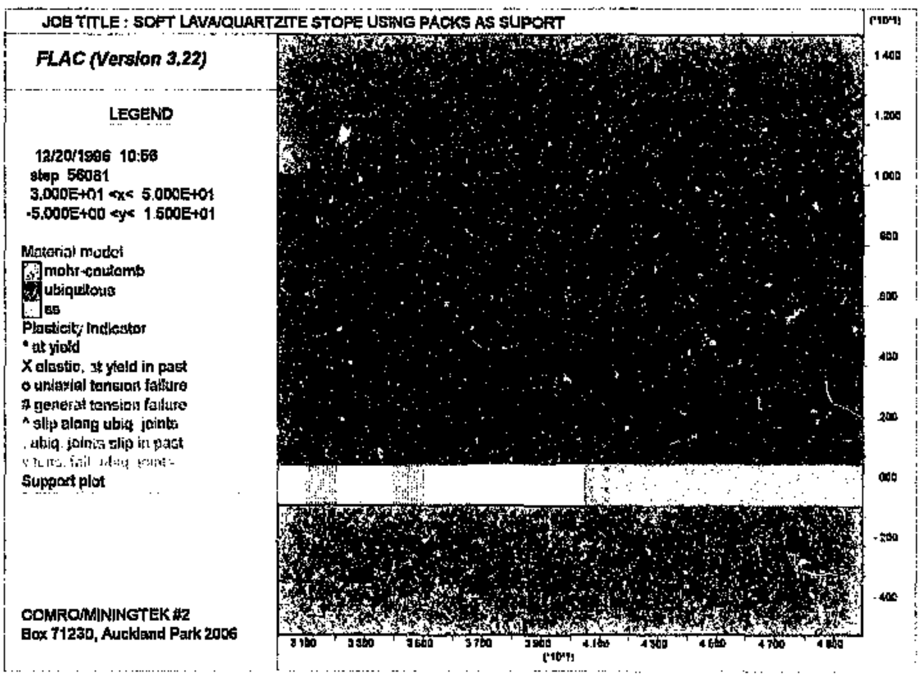


Figure 5.10. Model with timber packs as support.

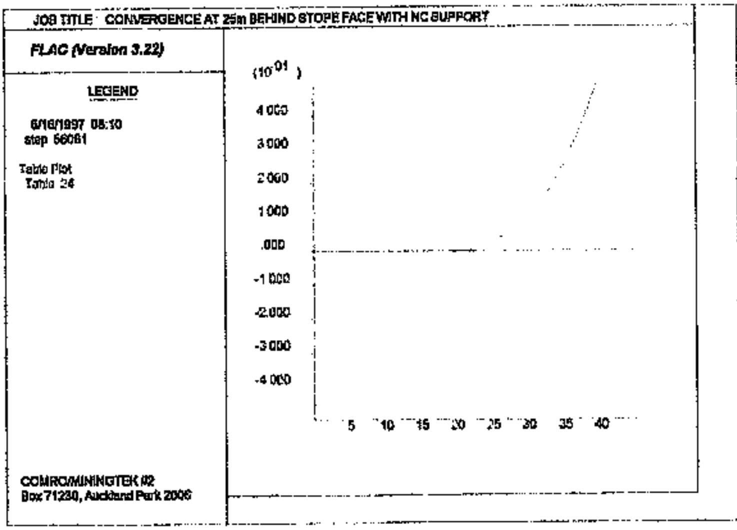


Figure 5.11a. Displacement between hangingwall and footwall monitored at 25 m behind the stope face with no support.

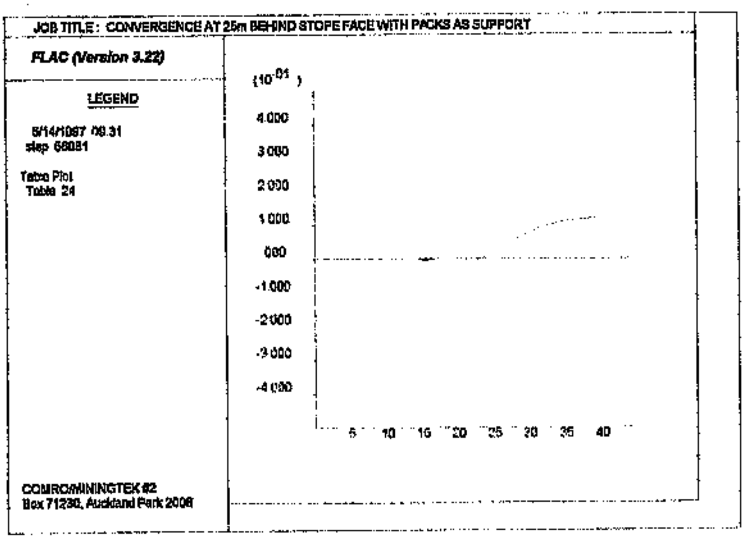


Figure 5.11b. Displacement between hangingwall and footwall monitored at 25 m behind the stope face with solid matpacks as support.

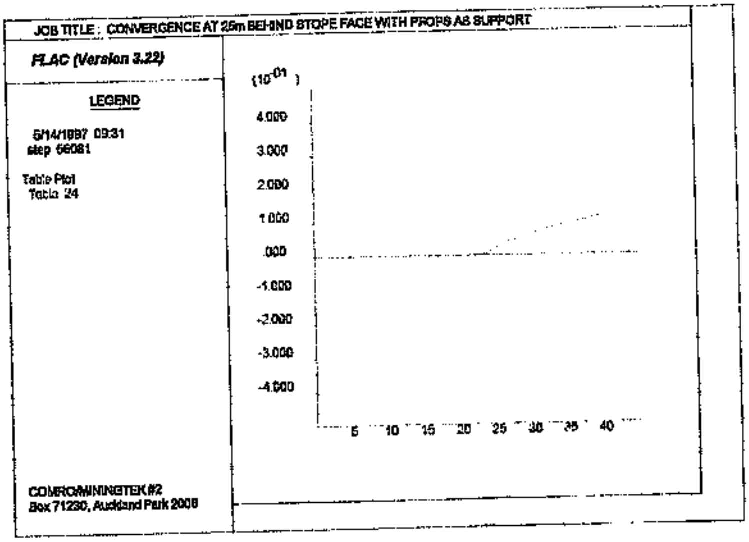


Figure 5.11c. Displacement between hangingwall and footwall monitored at 25 m behind the stope face with profile props as support.

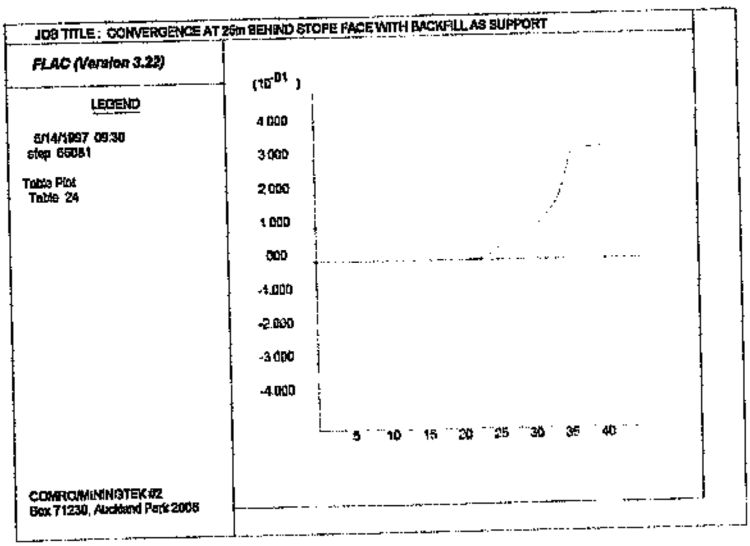


Figure 5.11d. Displacement between hangingwall and footwall monitored at 25 m behind the stope face with backfill (classified tailings, 48% porosity) as support.

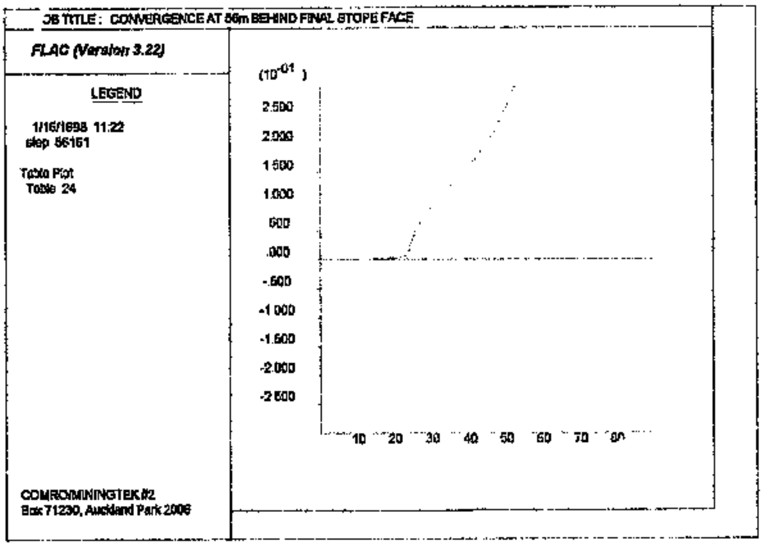


Figure 5.12a. Displacement between hangingwall and footwall monitored at 55 m behind the stope face with no support.

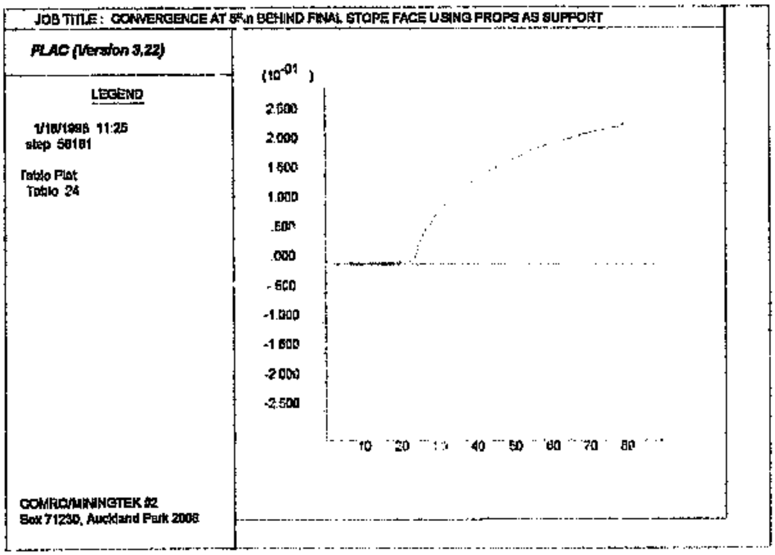


Figure 5.12b. Displacement between hangingwall and footwall monitored at 55 m behind the stope face with profile props as support.

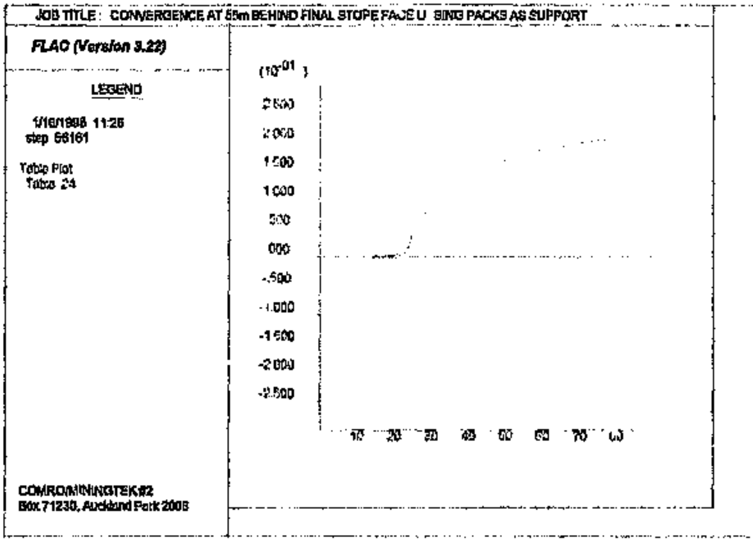


Figure 5.12c. Displacement between hangingwall and footwall monitored at 55 m behind the stope face with solid matpacks as support.

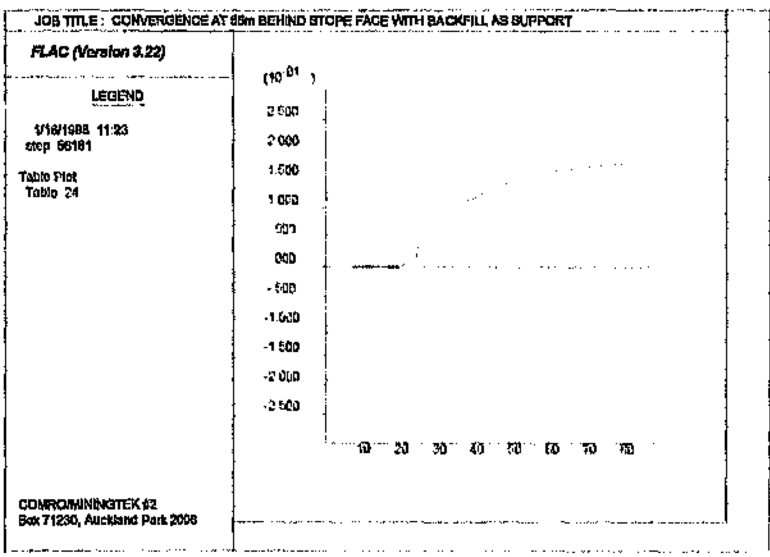


Figure 5.12d. Displacement between hangingwall and footwall monitored at 55 m behind the stope face with backfill as support.

## 5.6 Conclusion

From the analyses outlined above the Mohr-Coulomb with strain-softening proved most successful. The fracture angles are greatly affected by the onset of rock failure and subsequent softening. The development of areas of plastic failure is restricted to a few zones ahead, below and above the stope when the material properties obtained from laboratory tests are used directly. In general terms, the results from the analyses have indicated some reasonable representation of the rock mass at the geotechnical area on Kloof Gold Mine. It must however be mentioned that these are only preliminary results that provide the basis for a much more detailed future study. It is therefore recommended that further work be done to fully understand the mechanisms that are responsible for the observed rock mass behaviour.

# CHAPTER SIX

## CONCLUSIONS AND SUPPORT RECOMMENDATION

The results obtained from the site monitoring have shown that the rate of closure in this geotechnical area is below 5 mm/day. The analyses has further revealed that the back area support resistance starts to build up at about 7 m from the stope face. The extensometers showed that there is no significant separation of bedding-parallel discontinuities in the hangingwall and footwall. A reasonable representation of the rock mass behaviour has been achieved by using the conceptual model.

The general inclination of the mining induced fractures and the geological features has been presented in chapter four. The results have shown that the behaviour of the rock mass, is controlled by both geological features and mining induced stress fractures. The fracture orientation analyses have further confirmed that the rockfalls observed in the north panels are due to the unfavourable intersection of both geological features and mining induced stress fractures.

The reversed orientation of the mining induced fractures and their clustering around the ramp structures in the north panels, suggest that their formation is to some extent influenced by these geological structures. The hangingwall appears to be more stable when advancing towards SW than in the NE direction. This is illustrated in the figure 6.1 below.

Amidst the host of speculations that could be put across to explain these observations, the material properties of the soft lava are considered to contribute significantly to the observed behaviour. In situ stress measurements were not carried out during the study. Information about the pre and post-mining stress regimes could help understand this phenomenon.

Another factor that could influence the stability of the hangingwall is the installation of the timber packs. As illustrated in the figure 6.2 below, the support position could coincide with the region of fractured in the hangingwall in the southern stopes. In contrast, the support units appear to be installed slightly ahead of the fractured region, hence the rockfalls. The distribution of the thrust faults suggests that movements in the back area should be restricted to 10 m from the stope face.

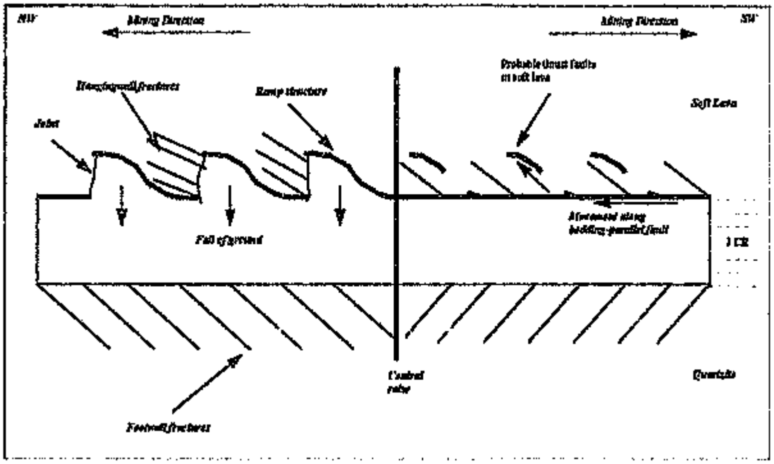


Figure 6.1. A simplified strike section showing the hangingwall conditions in both north and south panels.

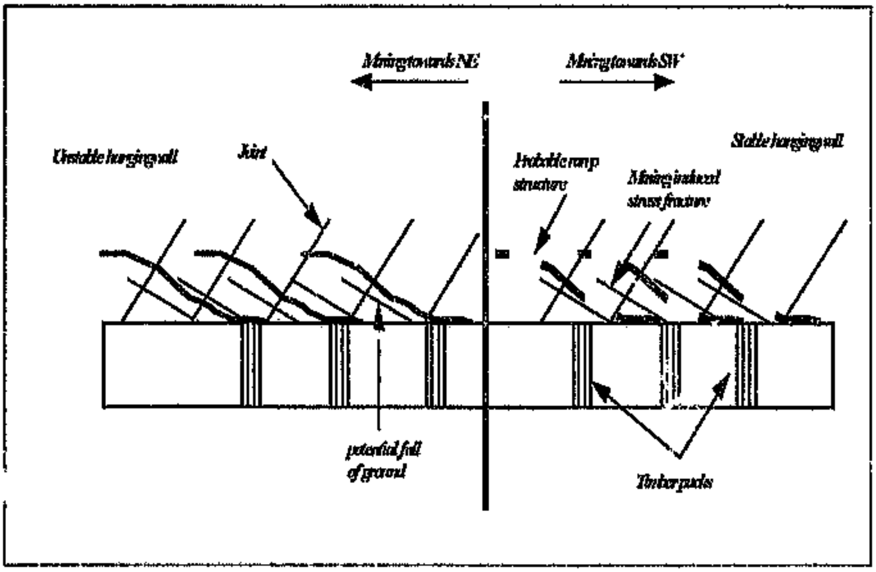


Figure 6.2. Positions of support units in relation to the fall out areas in both north and south panels.

The findings in the soft lava-quartzite geotechnical area are quite peculiar to this particular geological environment. Faulting appears to be a major factor influencing the stability of the hangingwall. It can be concluded from the study that in this geotechnical area, the design of support systems should take both geological features and mining induced fractures into consideration. The unstable condition of the hangingwall in the north panels suggests that a slight reduction in the strike spacing between support units could improve the hangingwall conditions. Flexibility should be incorporated into mine support standards to allow changes when the need arises. Thus in situations like this, it should be possible to apply different strike spacings in the south and north stopes.

Detailed investigations are recommended for future studies as this would further improve the understanding of the rock mass behaviour. These may include the following:

a). The influence of geological features on the orientation of mining induced stress fractures.

b). In situ stress measurements which could give an idea about the direction of the major principal stress.

c). The influence of the rate of face advance an[illegible] ld be investigated.

d). Further numerical modelling work to provide greater insight into the mechanics of fracture formation could be of interest.

# REFERENCES

1. Adams, G. R., and Jager, A. J. (1979). Petroscopic obse vations of fracturing of rock ahead of stope face in deep level gold mines. Unpubl. Report. Chamber of mines of South Africa, 20pp.

2. An industry Guide to Ameliorating Rockfalls and Rockburst (1988). COMRO.

3. Anonymous. Geology of Kloof Gold Mine.

4. Berlenbach, J. W. (1995). Aspects of bedding-parallel faulting associated with the Ventersdorp Contact Reef on the Kloof Gold Mine. S. Afr. J. Geol, 335 - 348.

5. Brummer, R. K. (1987). Fracturing and deformation at the edges of tabular gold mining excavations and the development of a numerical model describing such phenomena. Ph.D. Thesis Ra~ 'rikaans Univ., Johannesburg.

6. Brummer, R. K. & Rorke A. J. (1984). Mining induced Fracturing around deep gold mine stopes. C.O.M. of South Africa, Research Report No. 38/86.

7. Cundell P. (1986). FLAC Manual. Itasca Consulting.

8. Emere G., T., G. (1982). The development of stope-support technology in South African gold mines. Proceedings, 12th CMMI Congress. Johannesburg, S. Afr. Inst. Min. Metall. (or Geol. Soc. S. Afr.), 377 - 384.

9. Engelbrecht, C. J., Baumbach, G.W.S., Matthysen, J.L. & Fletcher, P. (1986). The West Wits Line. In : Anhaeusser, C. R. & Maske, S. (Eds.), Mineral Deposits of Southern Africa, I. Geol. Soc. S. Afri, Johannesburg, 599 - 648.

10. Eve R. A. (1985). VCR Project. SIMRAC Interim Report. CSIR Miningtek.

11. Fairhurst, C. & Cook, N. G. W (1966). The phenomenon of rock splitting parallel to the direction of maximum compression in the neighbourhood of a surface. Proc. First Cong. of Int. Soc. Rock Mech. Lisbon.

12. Gay N., C. and Jager A., J (1986). The influence of geological features on problems of rock mechanics in Witwatersrand mines. Minerals Deposits of Southern Africa. Geolo. Soc. S. Afr., Johannesburg, 753 - 772.

13. Gurtunca, R. G., Jager, A. J., Adams, D. J. and Gonlag, M. (1989). The insitu behaviour of backfill materials and the surrounding rock mass in South African gold mines. Symposium on Innovations on Mining Backfill Technology, Montreal, Canada, 187-197.

14. Hawkes, I. & Kwitowski, A. J. (1979). Mine Roof Borehole Extensometers, 20th U.S. Symposium on Rock Mechanics, Austin, Texas, 491 - 500.

15. Hodgson, K. (1967). The behaviour of the failed zone ahead of a face, as indicated by continuous seismic and convergence measurements. C.O.M. Research Report 31/67.

16. Hoek, E. & Bienlawski, Z. T. (1966). Fracture propagation mechanism in hard rock. Proc. First Cong. of Int. Soc. Rock Mech., Lisbon.

17. Hoek, E. and Brown, E. T. (1980). Graphical presentation of geological data. In Underground excavations in rock. London: Instn. Min. Metall, 61-86.

18. Jager A. J., Piper, P. S. & Gay, N. C. (1987). Rock Mechanics aspects of backfill in deep South African gold mines. Proc. 6th Int. Congress on Rock Mech., International Society for Rock Mechanics, Montreal, Canada.

19. Jager A. J. & Roberts M. K. C. (1986). Support Systems in Productive Excavations. GOLD 100. Proceedings of the International Conference on Gold. Volume 1: Gold Mining Technology. Johannesburg, SAIMM, 289 - 300.

20. Kersten, R. W. O (1969). Structural analysis of fractures around underground excavations on a Witwatersrand gold mine. MSc. Thesis. University of Pretoria.

21. Legge N. B. (1986). Rock deformation in the vicinity of deep gold mine stopes and its relation to fracture. C.O.M. of South Africa Research Report No. 14/86.

22. Piper, P., & Gurtunca, R. G. (1987). Measuring convergence and ride. SANGORM News, February, Johannesburg, editor R. Brummer, 14 - 15.

23. Ramsay, J.G. & Huber, M.I. (1987). The techniques of modern structural geology, II. Academic Press, London, 505 - 539.

24. Roering, C. & Smit, C.A. (1987). Bedding parallel shear, thrusting and quartz vein formation in Witwatersrand quartzites. J. Struct. Geol., 9, 419 - 427.

25. Salamon M., D., G., (1974). Rock Mechanics of underground excavations. Proc. 3rd Congr. Int. Soc. Rock Mech. Denver, Vol. 1, Part B, 951 - 1100.

26. Wagner H., (1975). The application of Rock Mechanics Principles to Strata Control in South African Gold Mines. Proceedings of the 10th Canadian Rock Mechanics Symposium, Kingston, September 2 - 4, 248 - 278.

## APPENDIX ONE

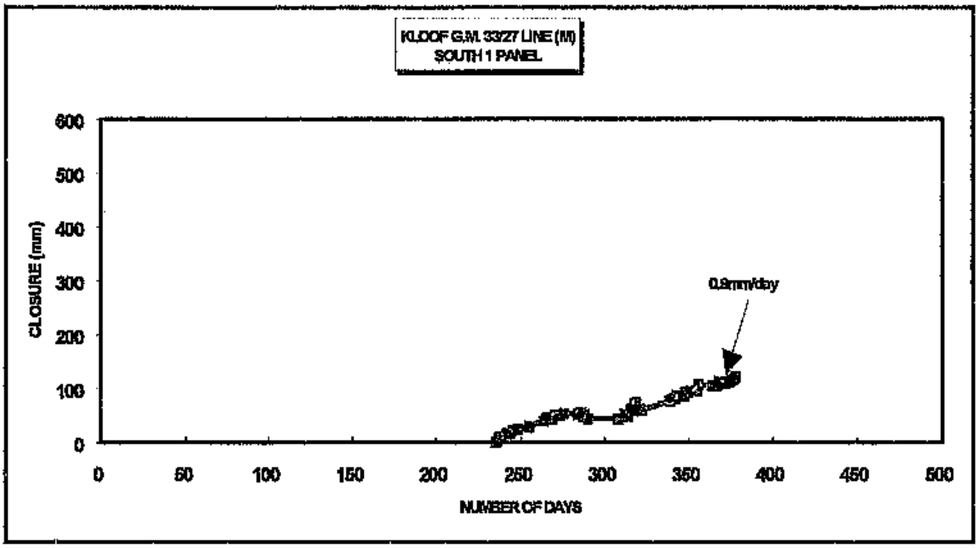


(a)

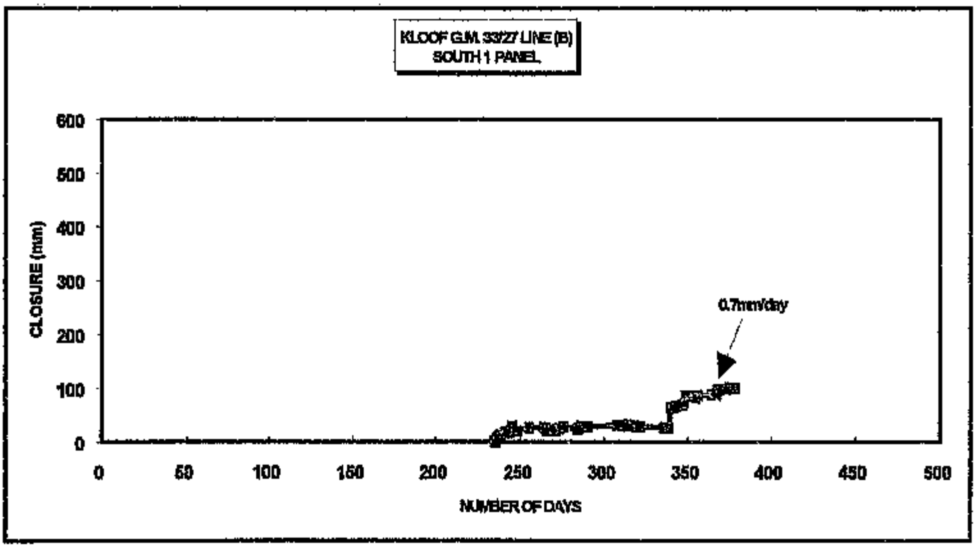


(b)

Diagram 1. Convergence results from Kloof Gold Mine, 33/27 longwall, South 1 Panel.

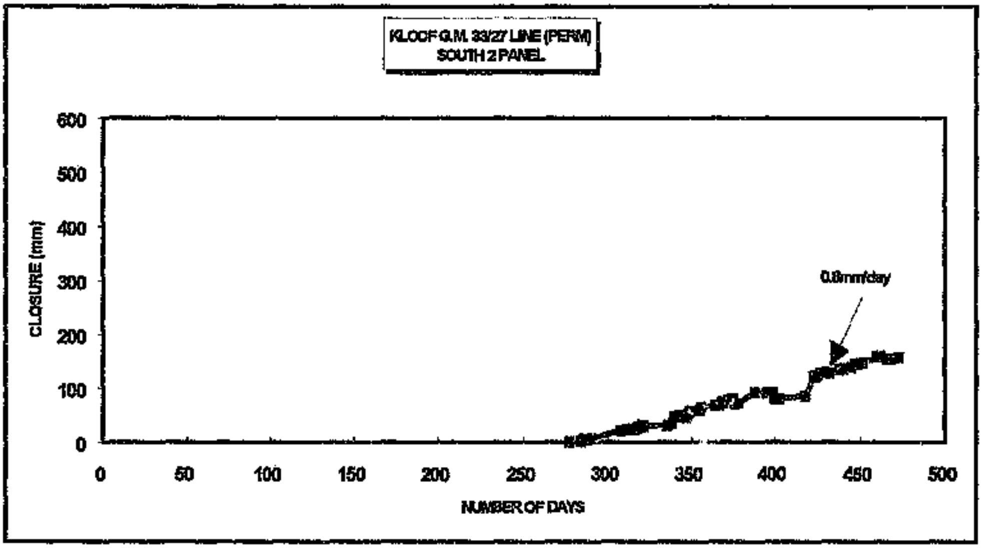


Diagram 2. Convergence results from Kloof Gold Mine, 33/27 longwall, South 2 Panel.

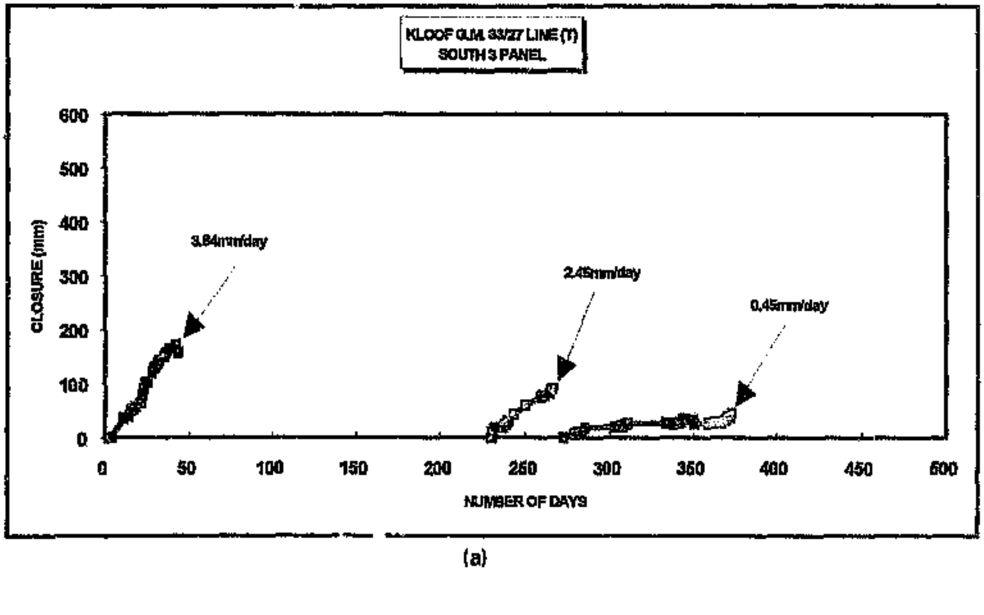


(a)

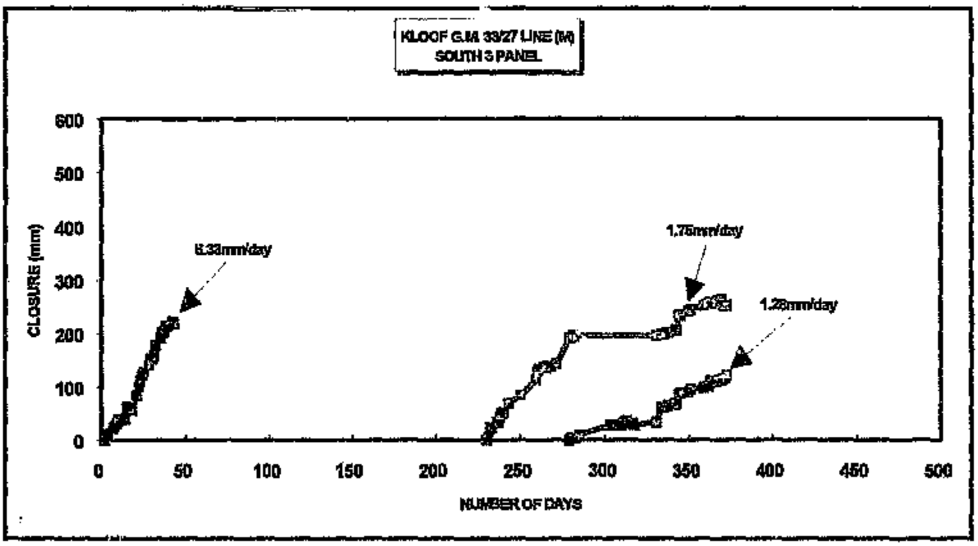
KLOOF G.M. 33/27 LINE (M)
SOUTH 3 PANEL
6.33mm/day
1.75mm/day
1.28mm/day
CLOSURE (mm)
NUMBER OF DAYS
0
100
200
300
400
500
600
0
50
100
150
200
250
300
350
400
450
500

(b)

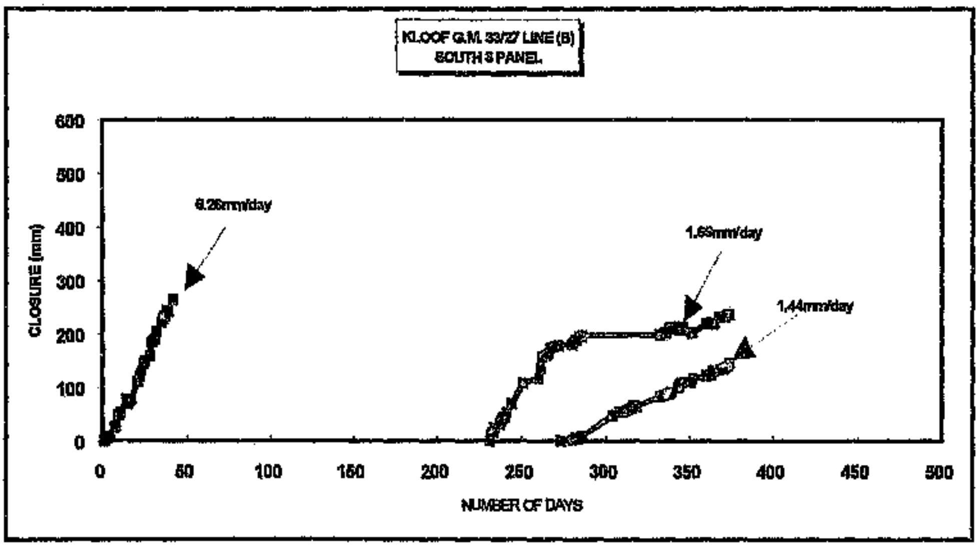
KLOOF G.M. 33/27 LINE (B)
SOUTH 3 PANEL
6.26mm/day
1.69mm/day
1.44mm/day
CLOSURE (mm)
NUMBER OF DAYS
0
100
200
300
400
500
600
0
50
100
150
200
250
300
350
400
450
500

(c)

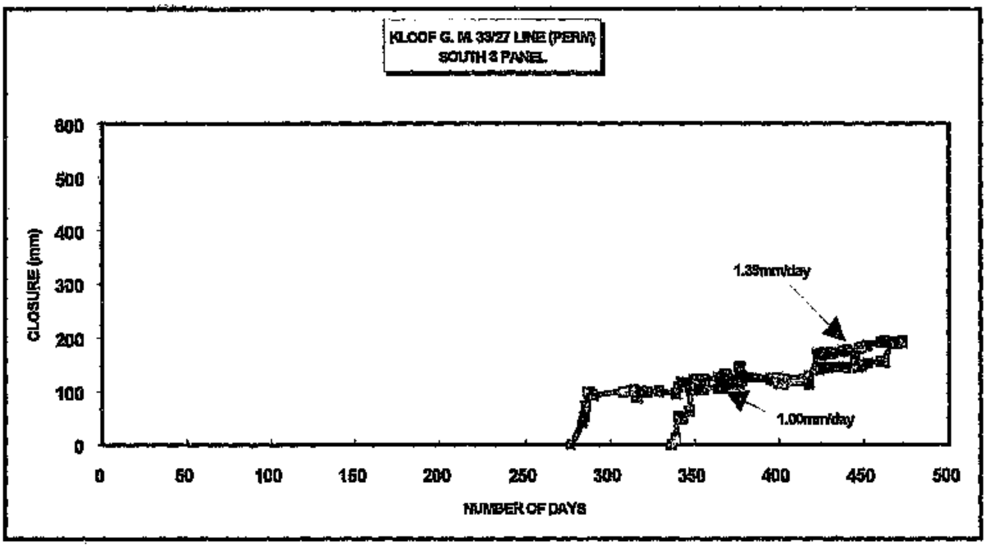


(d)

Diagram 3. Convergence results from Kloof Gold Mine, 33/27 longwall, South 3 Panel.

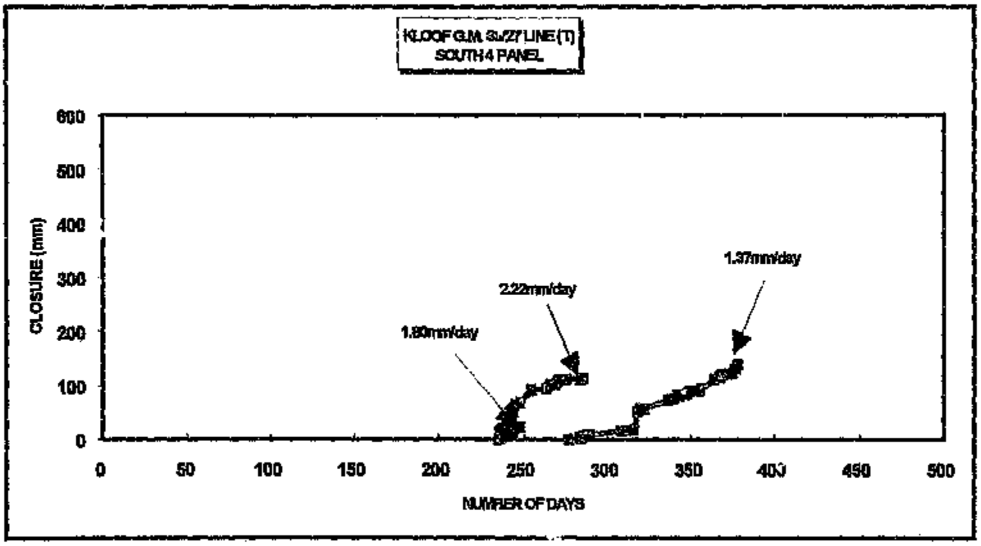


(a)

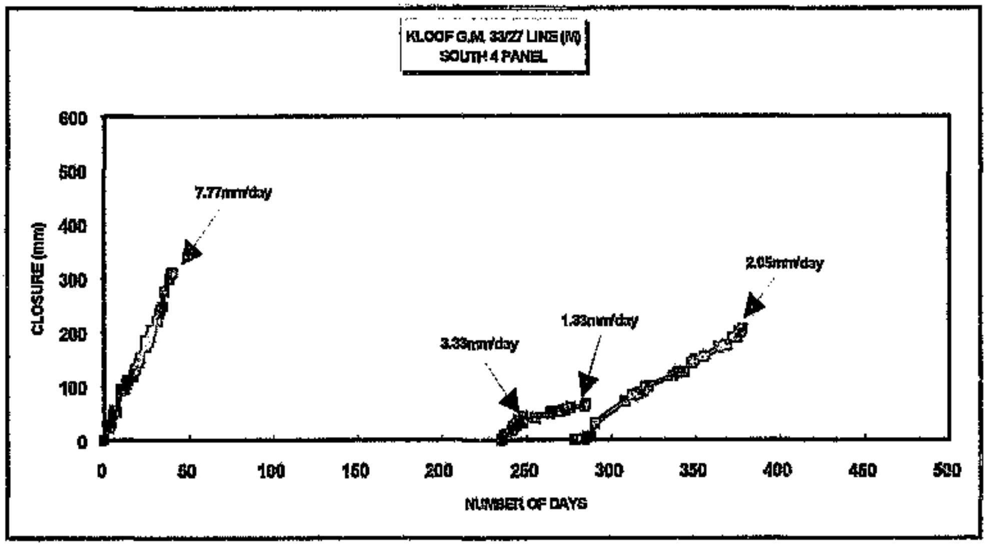
KLOOF G.M. 33/27 LINE (M)
SOUTH 4 PANEL
7.77mm/day
2.05mm/day
1.33mm/day
3.33mm/day
CLOSURE (mm)
NUMBER OF DAYS

(b)

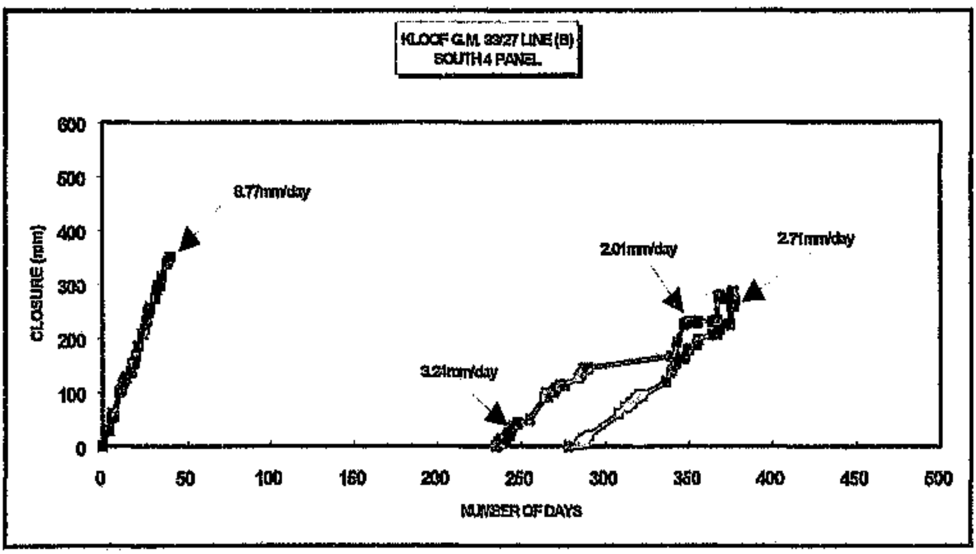
KLOOF G.M. 33/27 LINE (B)
SOUTH 4 PANEL
8.77mm/day
2.01mm/day
2.71mm/day
3.24mm/day
CLOSURE (mm)
NUMBER OF DAYS

(c)

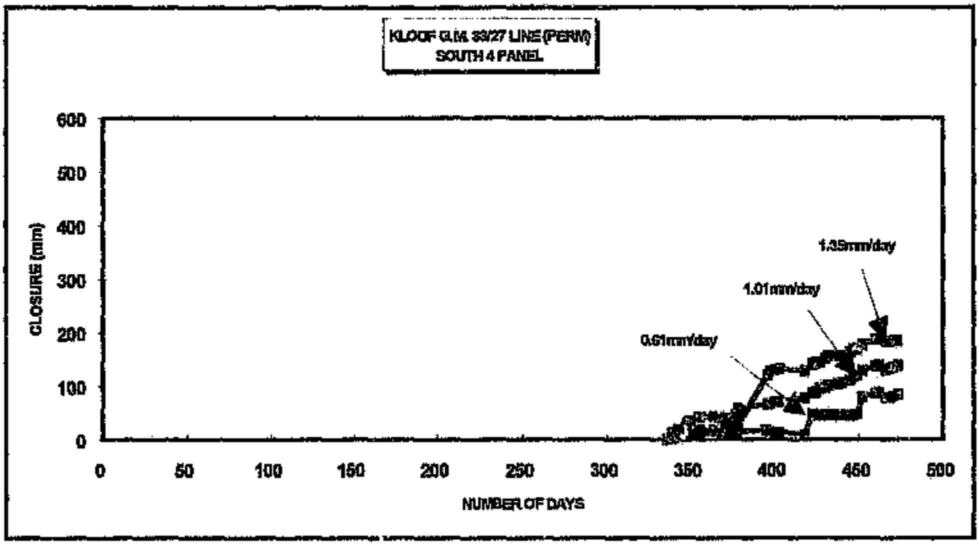


(d)

Diagram 4. Convergence results from Kloof Gold Mine, 33/27 longwall, South 4 Panel.

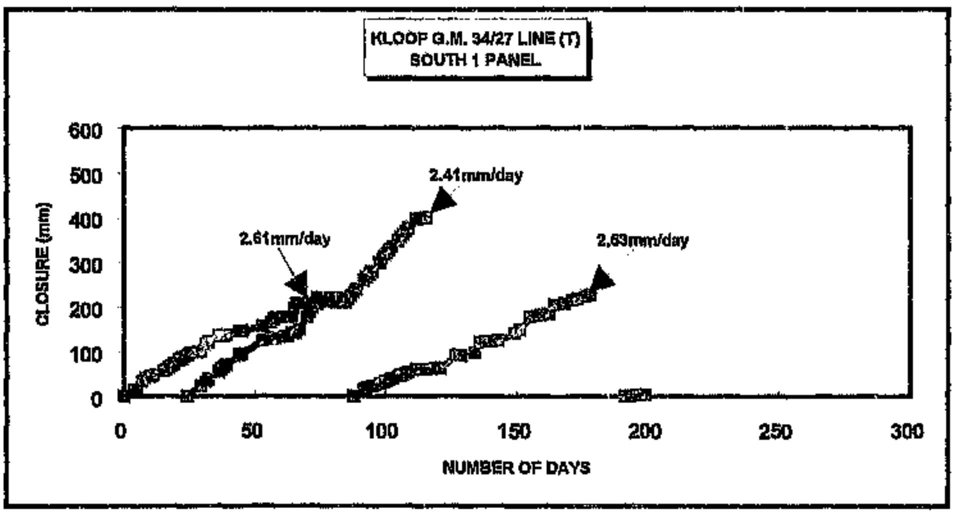


(a)

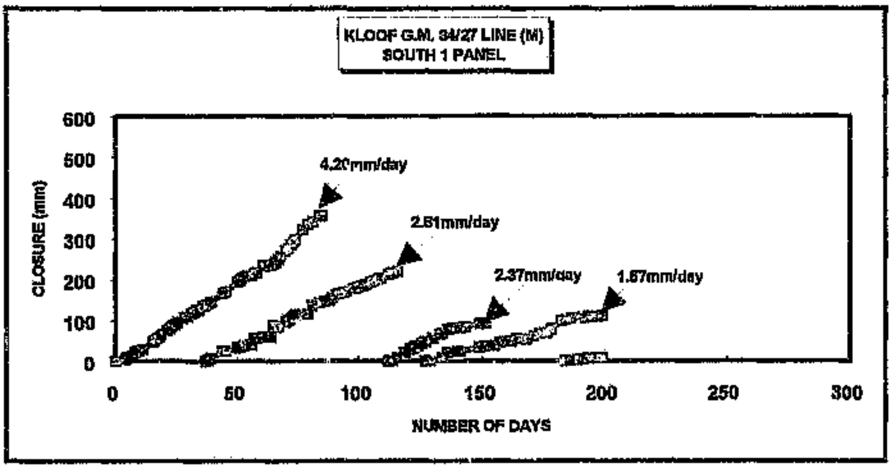
KLOOF G.M. 34/27 LINE (M)
SOUTH 1 PANEL
CLOSURE (mm)
NUMBER OF DAYS
4.20mm/day
2.61mm/day
2.37mm/day
1.67mm/day
0
100
200
300
400
500
600
0
50
100
150
200
250
300

(b)

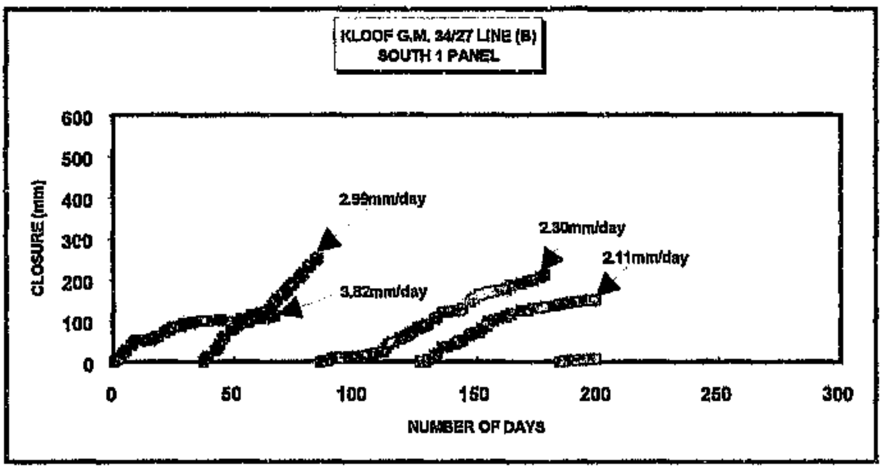
KLOOF G.M. 34/27 LINE (B)
SOUTH 1 PANEL
CLOSURE (mm)
NUMBER OF DAYS
2.99mm/day
2.30mm/day
2.11mm/day
3.82mm/day
0
100
200
300
400
500
600
0
50
100
150
200
250
300

(c)

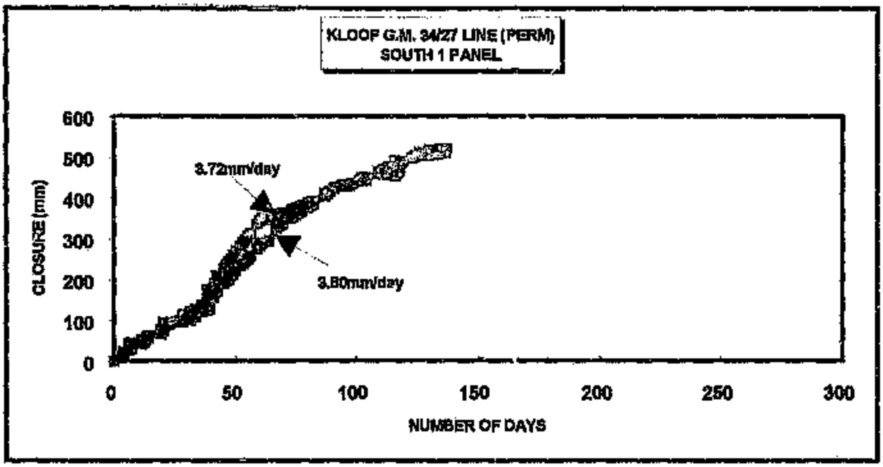


(d)

Diagram 5. Convergence results from Kloof Gold Mine, 34/27 longwall, South 1 Panel

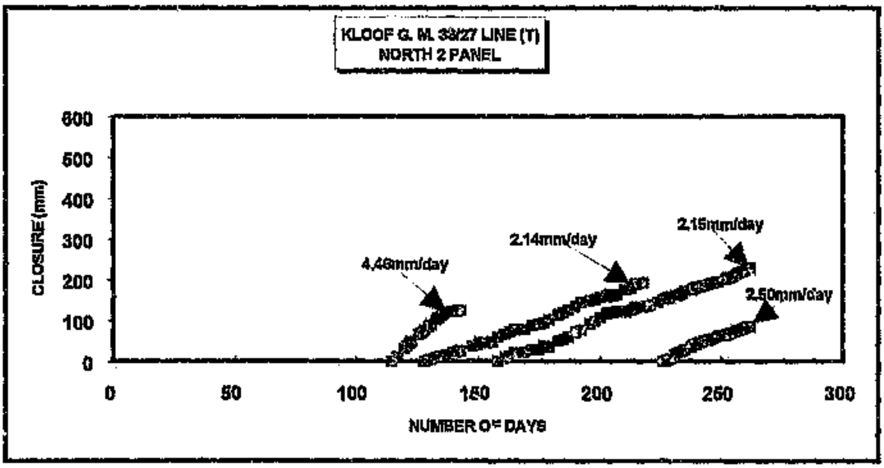


(a)

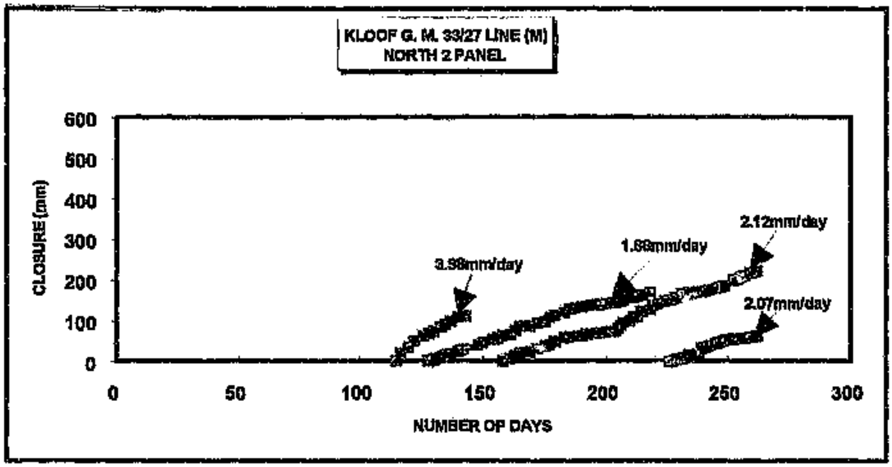
KLOOF G. M. 33/27 LINE (M)
NORTH 2 PANEL
CLOSURE (mm)
NUMBER OF DAYS
3.98mm/day
1.69mm/day
2.12mm/day
2.07mm/day

(b)

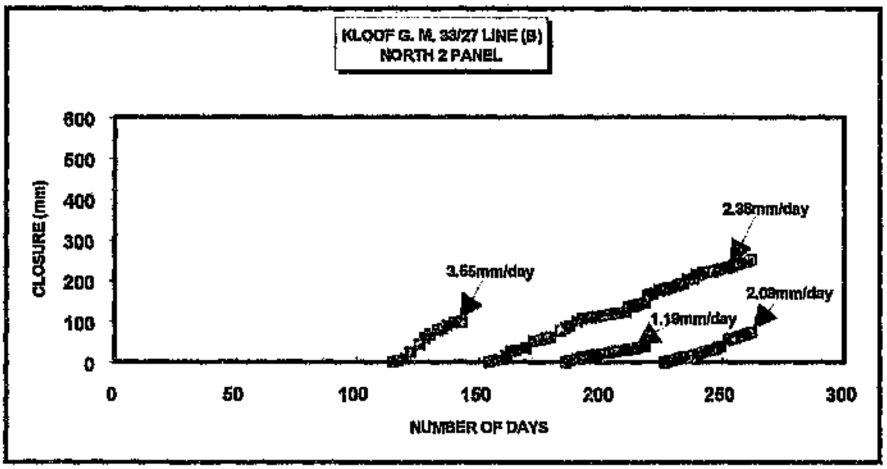
KLOOF G. M. 33/27 LINE (B)
NORTH 2 PANEL
CLOSURE (mm)
NUMBER OF DAYS
3.65mm/day
2.38mm/day
1.19mm/day
2.09mm/day

(c)

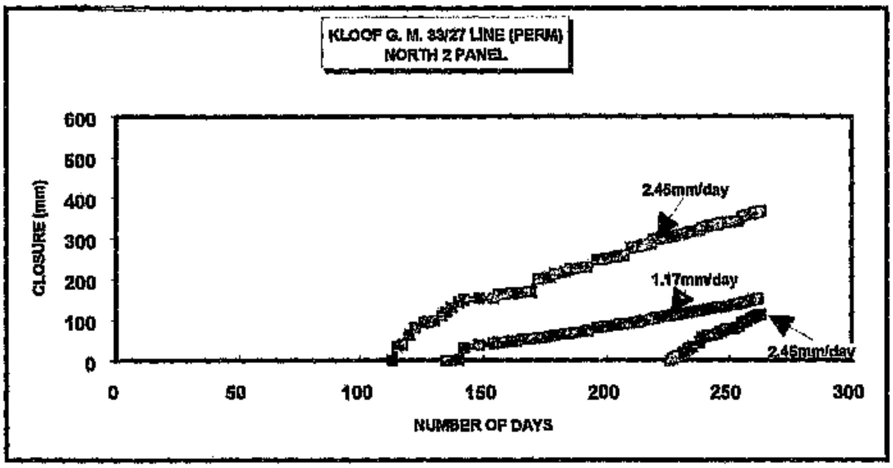

(d)

Diagram 6. Convergence results from Kloof Gold Mine, 33/27 longwall, North 2 Panel.

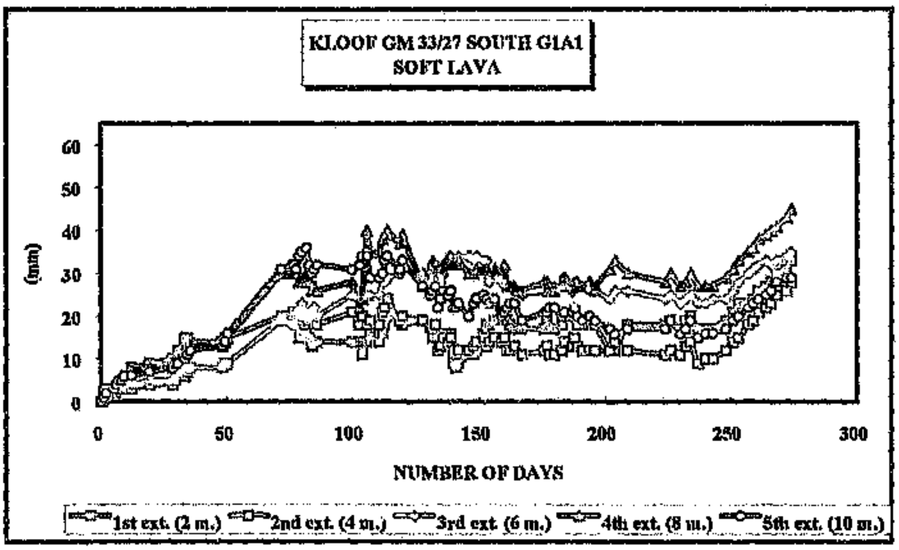

(a)

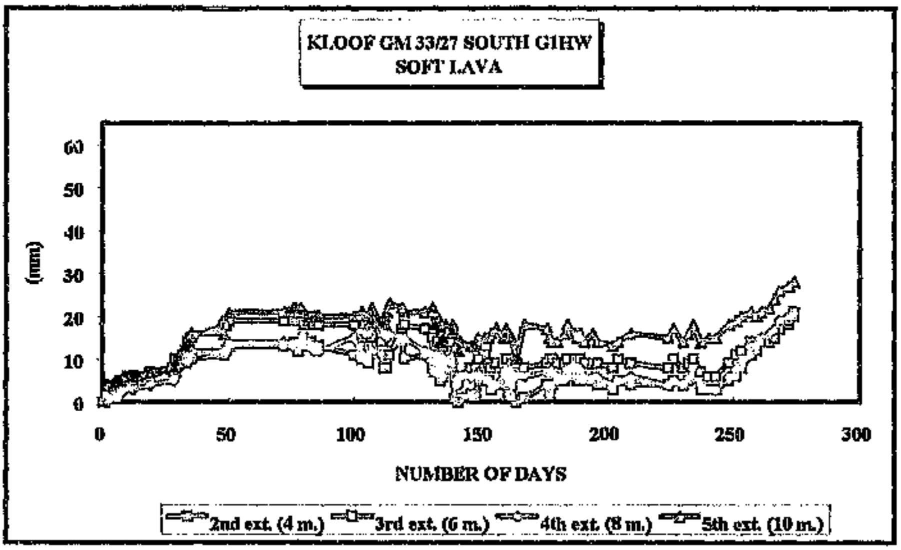


(b)

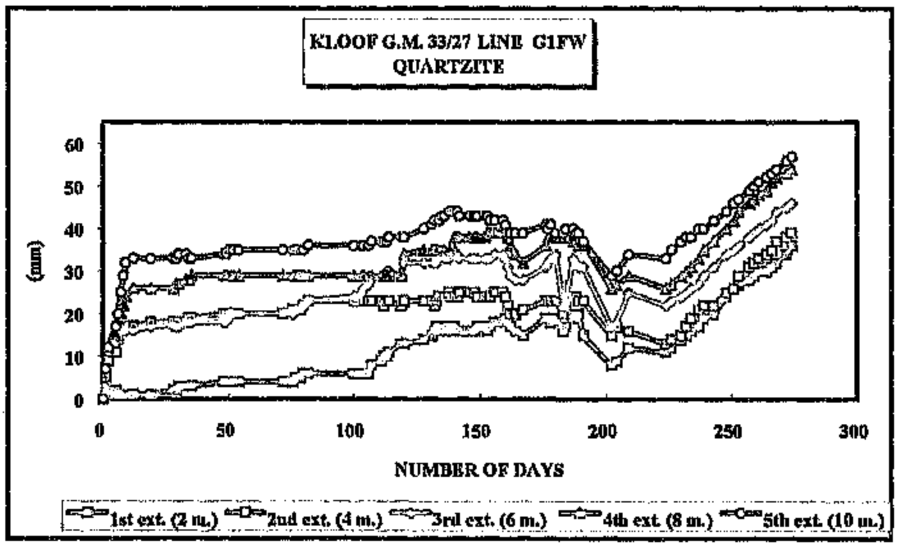


(c)

Diagram 7. Extensometer results from Kloof Gold Mine, 3 Shaft on 33 Level 27 Line in South 1 panel.

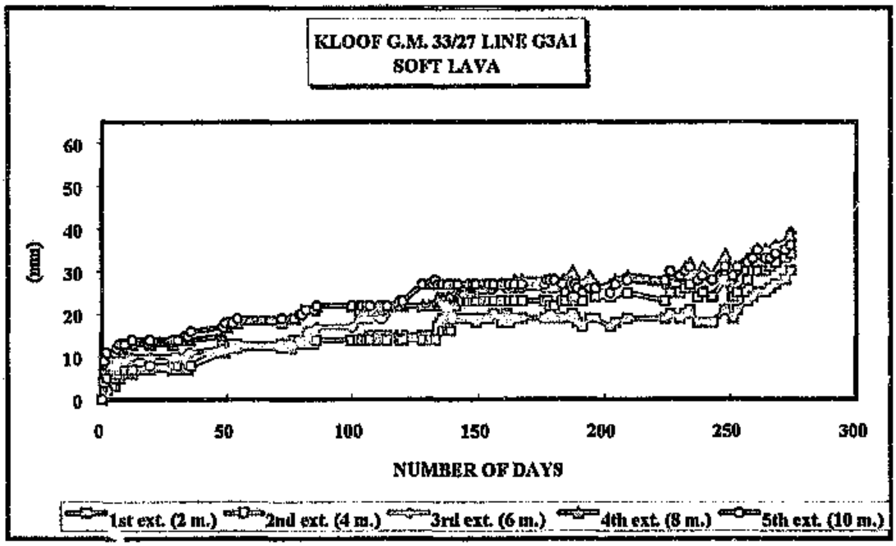
KLOOF G.M. 33/27 LINE G3A1
SOFT LAVA
60
50
40
30
20
10
0
(mm)
0
50
100
150
200
250
300
NUMBER OF DAYS
1st ext. (2 m.)
2nd ext. (4 m.)
3rd ext. (6 m.)
4th ext. (8 m.)
5th ext. (10 m.)

(a)

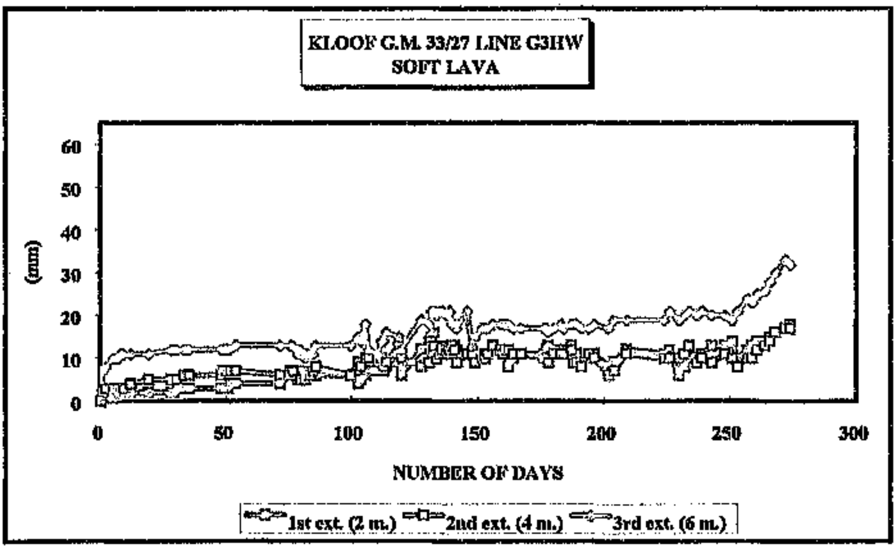
KLOOF G.M. 33/27 LINE G3HW
SOFT LAVA
60
50
40
30
20
10
0
(mm)
0
50
100
150
200
250
300
NUMBER OF DAYS
1st ext. (2 m.)
2nd ext. (4 m.)
3rd ext. (6 m.)

(b)

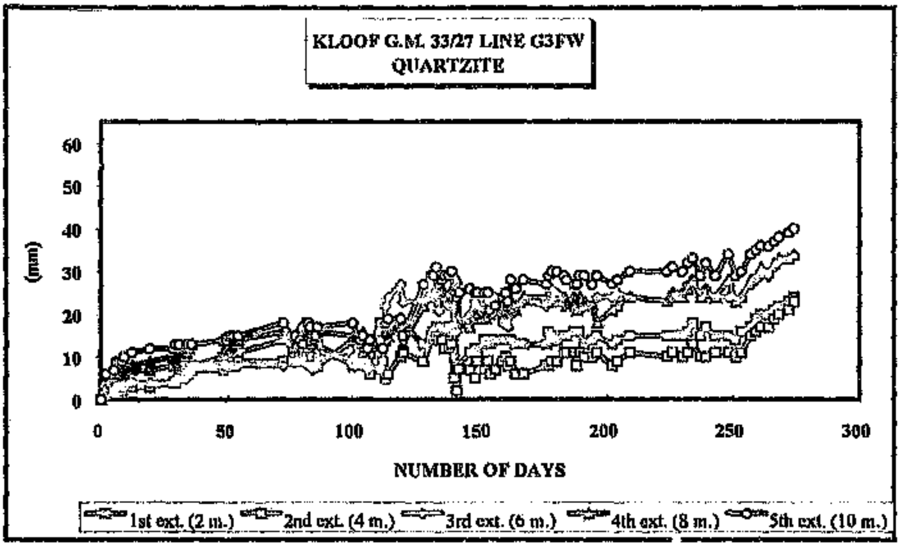


(c)

Diagram.8. Extensometer results from Kloof Gold Mine, 3 Shaft on 33 Level 27 Line in South 3 panel.

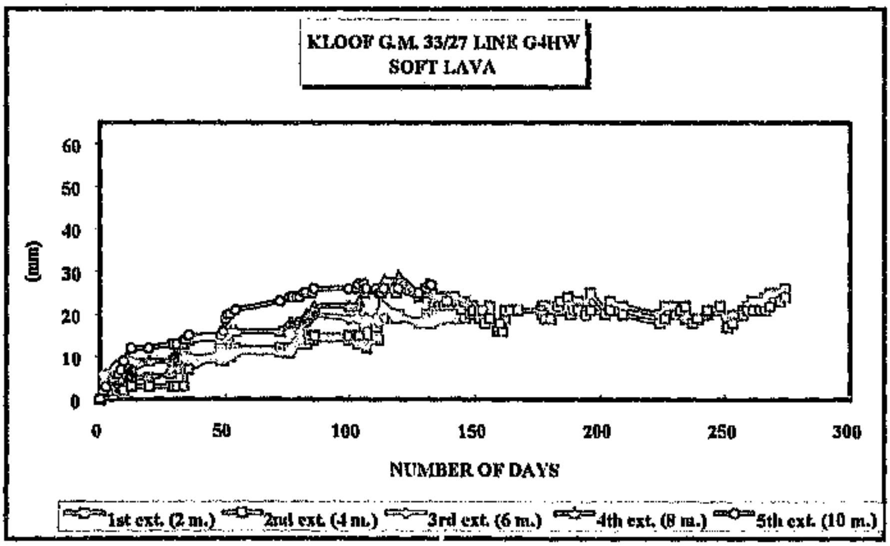


(e)

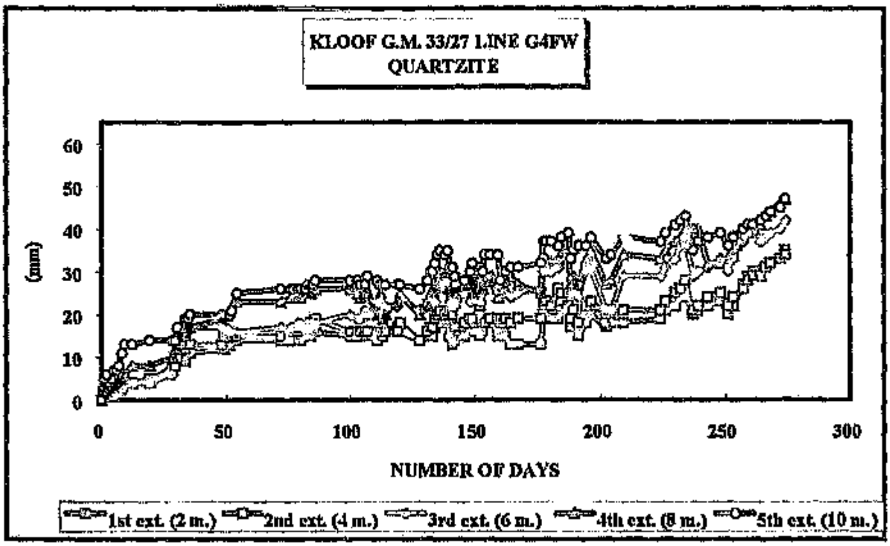


(b)

Diagram 9. Extensometer results from Kloof Gold Mine, 3 Shaft on 33 Level 27 Line in South 4 panel.